

Supporting Information

Synthesis, characterization and second-order nonlinear optical behaviour of ferrocene-diketopyrrolopyrrole dyads. Effect of alkene vs alkyne linkers

Sarbjeeet Kaur,^a Nick Van Steerteghem,^b Paramjit Kaur,*^a Koen Clays^b and Kamaljit Singh*,^a

^a*Department of Chemistry, UGC Centre of Advanced Study-II, Guru Nanak Dev University, Amritsar-143005, India. Email: kamaljit.chem@gndu.ac.in*

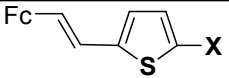
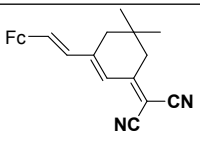
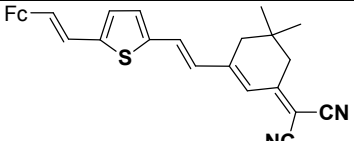
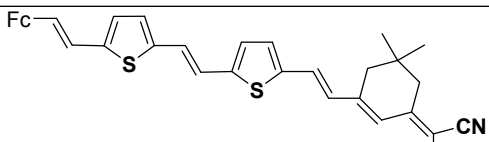
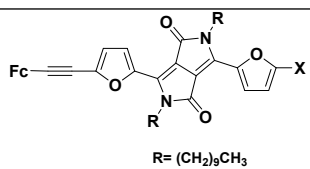
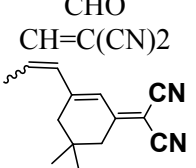
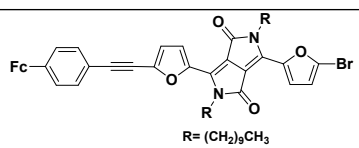
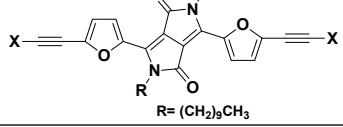
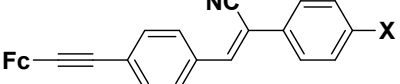
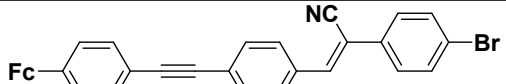
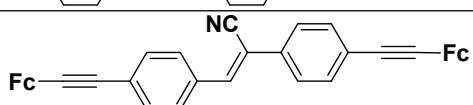
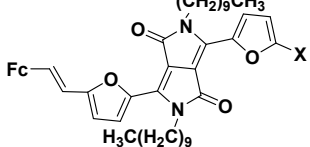
^b*Department of Chemistry, University of Leuven, Celestijnenlaan 200D, B-3001 Leuven, Belgium. E-mail: Koen.Clays@fys.kuleuven.be*

Sr. No.	Content	Page No.
1.	Table S1. Comparison of first hyperpolarizability, β_{HRS} (Literature vs. Present report).	S4-S5
2.	Figure S1. Thermogravimetric (TGA) curves of dyads 5a-c .	S6-S7
3.	Figure S2. UV-visible spectra of dyad 5a in dichloromethane and resolved peaks after band-fitting. (Black: experimental, Green: fitted curve)	S8
4.	Figure S3. UV-visible spectra of dyad 5b in dichloromethane and resolved peaks after band-fitting. (Black: experimental, Green: fitted curve)	S9
5.	Figure S4. UV-visible spectra of dyad 5c in dichloromethane and resolved peaks after band-fitting. (Black: experimental, Green: fitted curve)	S10
6.	Figure S5. Contour surfaces of frontier molecular orbitals of dyads 5a-c derived from TD-DFT at B3LYP/ 6-31G basis set (Iso-surface value= 0.02).	S11
7.	Figure S6. Spectro-electrochemical curve of chromophore 5b recorded at 1×10^{-5} M in dichloromethane.	S12
8.	Figure S7. Spectro-electrochemical curve of chromophore 5c recorded at 1×10^{-5} M in dichloromethane.	S12
9.	Figure S8. Linear correlation between the optical gap E_g^{opt} , determined from UV/CV and TD-DFT for the dyads 5a-c .	S13
10.	Table S2. Energies of the Frontier Orbitals (eV) HOMO-n to LUMO+n (n=0-6) obtained from TD-DFT carried out at B3LYP/6-31G level in dichloromethane as solvent medium.	S13
11.	Table S3. Energies of the Frontier Orbitals (eV) HOMO-n to LUMO+n (n=0-6) obtained from TD-DFT carried out at B3LYP/6-31G level in gas phase.	S14
12.	Figure S9. B3LYP/6-31G predicted orbital energy level diagram for the dyads 5a-c .	S14
13.	Figure S10. Linear correlation of absorbance and concentration of 5a at 606 nm.	S15
14.	Figure S11. Linear correlation of absorbance and concentration of 5b at 640 nm.	S15
15.	Figure S12. Linear correlation of absorbance and concentration of 5c at 640 nm.	S16
16.	Table S4. Comparison of experimentally (UV-visible) and theoretically (TD-DFT) calculated absorption bands and assignment of electronic transitions for the dyads 5a-c .	S16-S17
17.	Figure S13. Contour surfaces of frontier molecular orbitals involved in LE electronic transitions of the dyad 5a obtained from TD-DFT calculations using dichloromethane as solvent at an iso-surface value of 0.02 au.	S18
18.	Figure S14. Contour surfaces of frontier molecular orbitals involved in HE electronic transitions of the dyad 5a obtained from TD-DFT calculations using dichloromethane as solvent at an iso-surface value of 0.02 au.	S19
19.	Figure S15. Contour surfaces of frontier molecular orbitals involved in LE electronic transitions of the dyad 5b obtained from TD-DFT calculations using dichloromethane as solvent at an iso-surface value of 0.02 au.	S20
20.	Figure S16. Contour surfaces of frontier molecular orbitals involved in HE electronic transitions of the dyad 5b obtained from TD-DFT calculations using dichloromethane as solvent at an iso-surface value of 0.02 au.	S21
21.	Figure S17. Contour surfaces of frontier molecular orbitals involved in LE electronic transitions of the dyad 5c obtained from TD-DFT calculations using dichloromethane as solvent at an iso-surface value of 0.02 au.	S22
22.	Figure S18. Contour surfaces of frontier molecular orbitals involved in HE electronic transitions of the dyad 5c obtained from TD-DFT calculations using dichloromethane as solvent at an iso-surface value of 0.02 au.	S23

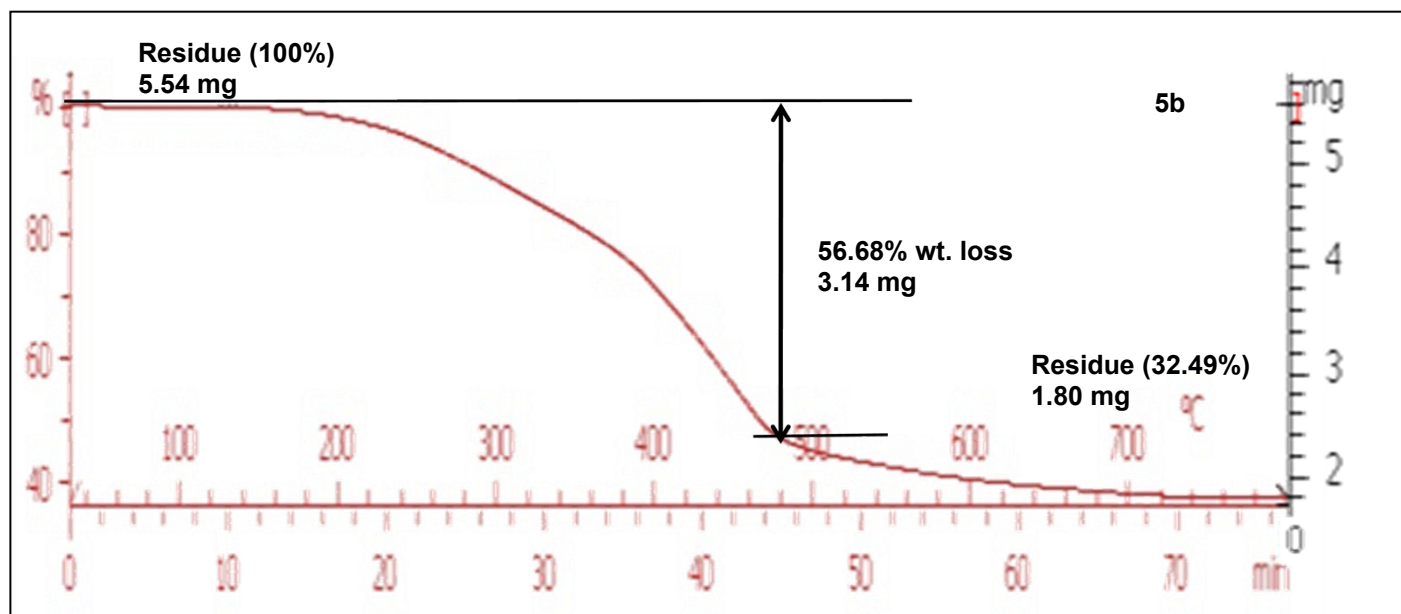
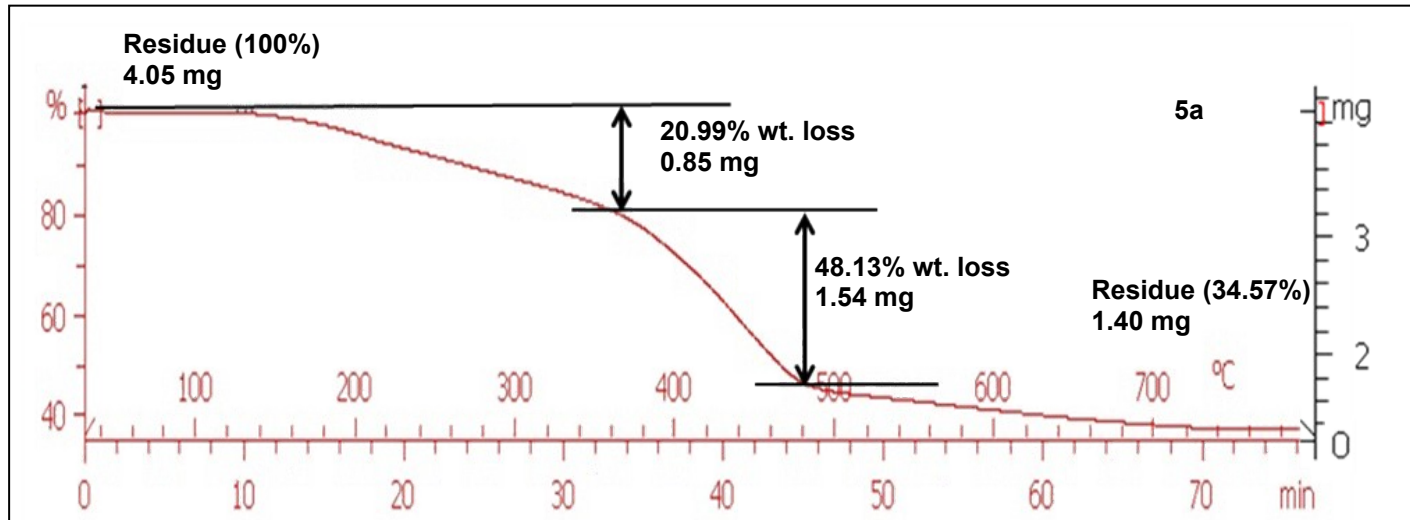
23.	Figure S19. Electron density maps of dyads 5a-c with iso-value of 0.0004.	S24
24.	Table S5. UV-visible data of 5a-c in various solvents.	S25
25.	Figure S20. Emission spectra of 5a at 1×10^{-5} in DCM at $\lambda_{\text{ex}} = 332$ nm.	S26
26.	Figure S21. Emission spectra of 5b at 1×10^{-5} in DCM at $\lambda_{\text{ex}} = 328$ nm.	S26
27.	Figure 22a. Emission spectra of 5c at 1×10^{-5} in DCM at $\lambda_{\text{ex}} = 286$ nm.	S27
28.	Figure 22b. Emission spectra of 5c at 1×10^{-5} in DCM at $\lambda_{\text{ex}} = 360$ nm.	S27
29.	Figure S23. ^1H NMR of 2 (CDCl ₃ , 500 MHz).	S28
30.	Figure S24. ^{13}C NMR of 2 (CDCl ₃ , 500 MHz).	S29
31.	Figure S25. ^1H NMR of 3 (CDCl ₃ , 500 MHz).	S30
32.	Figure S26. ^{13}C NMR of 3 (CDCl ₃ , 500 MHz).	S31
33.	Figure S27. ^1H NMR of 7 (CDCl ₃ , 500 MHz).	S32
34.	Figure S28. ^{13}C NMR of 7 (CDCl ₃ , 500 MHz).	S33
35.	Figure S29. ^1H NMR of 5a (CDCl ₃ , 500 MHz).	S34
36.	Figure S30. ^{13}C NMR of 5a (CDCl ₃ , 500 MHz).	S35
37.	Figure S31. ^1H NMR of 5b (CDCl ₃ , 500 MHz).	S36
38.	Figure S32. ^{13}C NMR of 5b (CDCl ₃ , 500 MHz).	S37
39.	Figure S33. ^1H NMR of 5c (CDCl ₃ , 500 MHz).	S38
40.	Figure S34. ^{13}C NMR of 5c (CDCl ₃ , 500 MHz).	S39
41.	Table S6. Cartesian co-ordinates of optimized geometry (B3LYP/6-31G) of 5a .	S39-S42
42.	Table S7. Cartesian co-ordinates of optimized geometry (B3LYP/6-31G) of 5b .	S42-S44
43.	Table S8. Cartesian co-ordinates of optimized geometry (B3LYP/6-31G) of 5c .	S44-S47
44.	Complete reference 75 .	S47

Table S1. Comparison of first hyperpolarizability, β_{HRS} (Literature vs Present report).

Chromophores	X	β_{HRS} (10^{-30} esu)	References
	H CN CHO	- 203 -	J.C. Calabrese, L.-T. Cheng, J.C. Green, S.R. Marder, W. Tam, <i>J. Am. Chem. Soc.</i> , 113 , 1991, 7227.
		21	
	Cr(CO) ₅ Mo(CO) ₅ W(CO) ₅	63 95 101	J. Mata, S. Uriel, E. Peris, R. Llusar, S. Houbrechts and A. Persoons, <i>J. Organomet. Chem.</i> , 562 , 1998, 197.
		40	J.A. Mata, E. Peris, I. Asselberghs, R. Van Boxel, A. Persoons, <i>New J. Chem.</i> , 25 , 2001, 1043.
		-	
		56	
		47	
		121	B.J. Coe, R.J. Docherty, S.P. Foxon, E.C. Harper, M. Helliwell, J. Raftery, K. Clays, E. Franz, B.S. Brunschwig, <i>Organometallics</i> , 28 , 2009, 6880.
		317	
		139	
		80	
		100	B. J. Coe, J. Fielden, S.P. Foxon, I. Asselberghs, K. Clays, S. van Cleuvenbergen, B.S. Brunschwig, <i>Organometallics</i> , 30 , 2011, 5731.

	CHO CN	83 54	P. Kaur, M. Kaur, G. Depotter, S. Van Cleuvenbergen, I. Asselberghs, K. Clays and K. Singh, <i>J. Mater. Chem.</i> , 2012, 22 , 10597.
		24	
		75	P. Kaur, M. Kaur, G. Depotter, S. Van Cleuvenbergen, I. Asselberghs, K. Clays and K. Singh, <i>J. Mater. Chem.</i> , 2012, 22 , 10597.
		120	P. Kaur, M. Kaur, G. Depotter, S. Van Cleuvenbergen, I. Asselberghs, K. Clays and K. Singh, <i>J. Mater. Chem.</i> , 2012, 22 , 10597.
 R= (CH ₂) ₉ CH ₃	CHO CH=C(CN)2 	207 303 913	S. Kaur, S. Dhoun, G. Depotter, P. Kaur, K. Clays and K. Singh, <i>RSC Adv.</i> , 2015, 5 , 84643.
 R= (CH ₂) ₉ CH ₃		173	
 R= (CH ₂) ₉ CH ₃	Fc Fc-C ₆ H ₄ -	152 160	
	Br CN CHO	110 146 183	S. Dhoun, G. Depotter, S. Kaur, P. Kaur, K. Clays and K. Singh, <i>RSC Adv.</i> , 2016, 6 , 50688.
		182	
		124	
 R= (CH ₂) ₉ CH ₃	Br CHO -C ₆ H ₄ CHO	115 150 231	This report

Thermogravimetric Curves



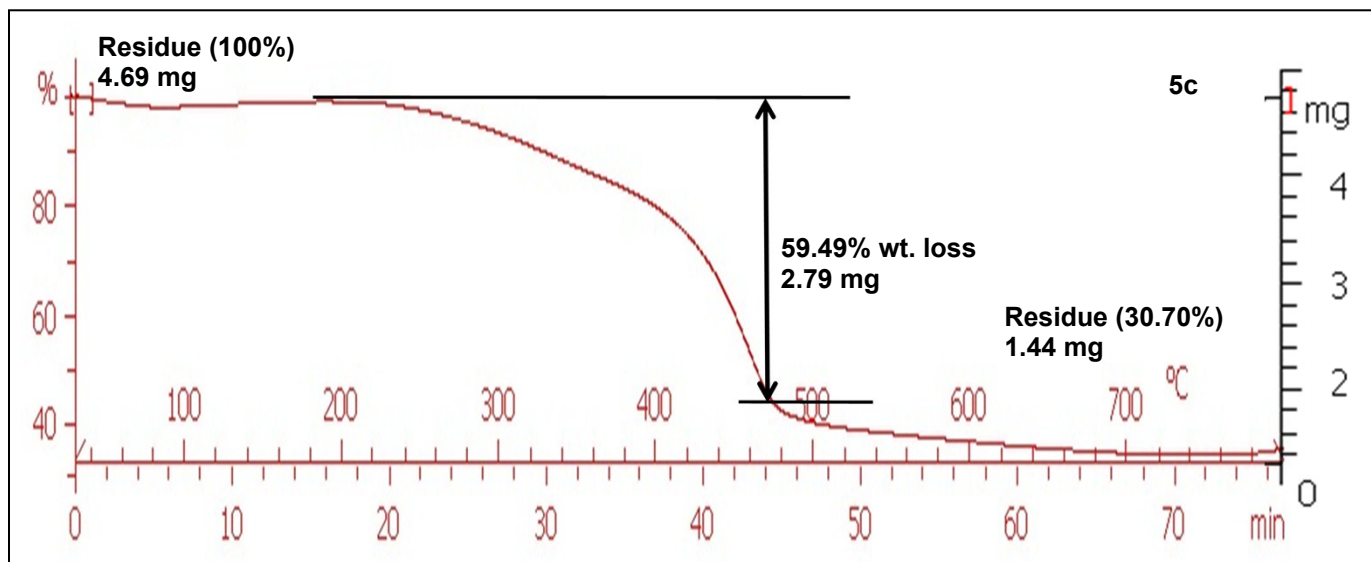


Figure S1. Thermogravimetric (TGA) curves of dyads **5a-c**.

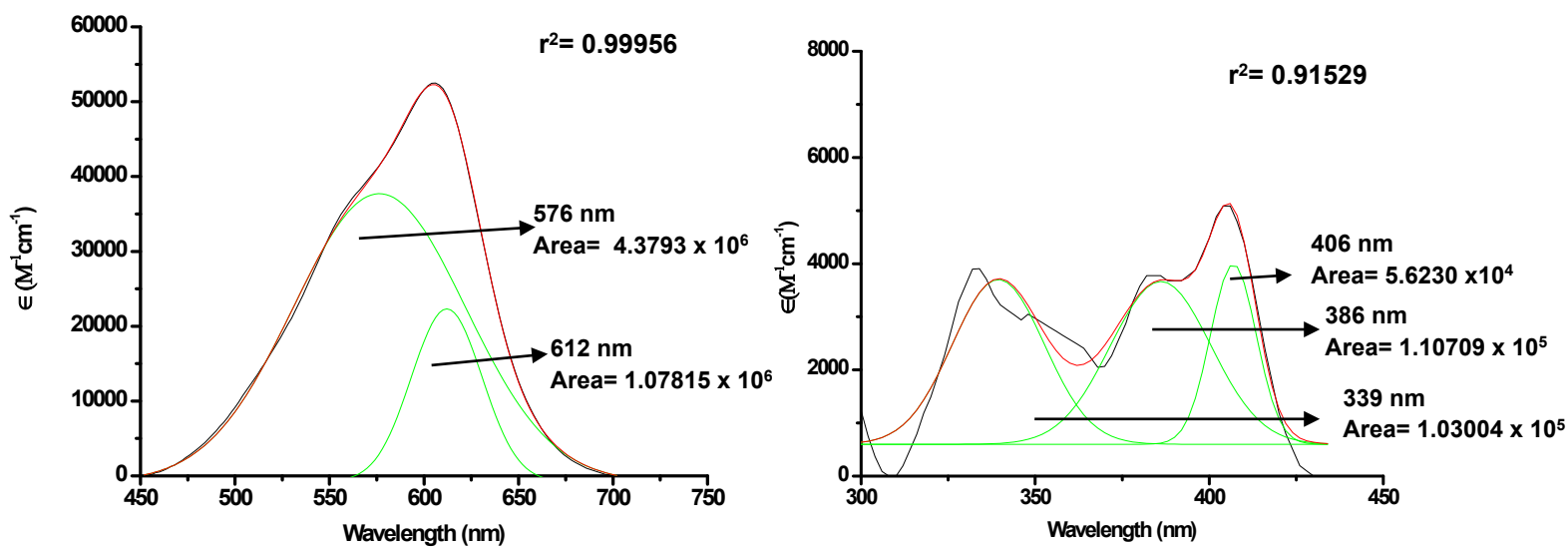
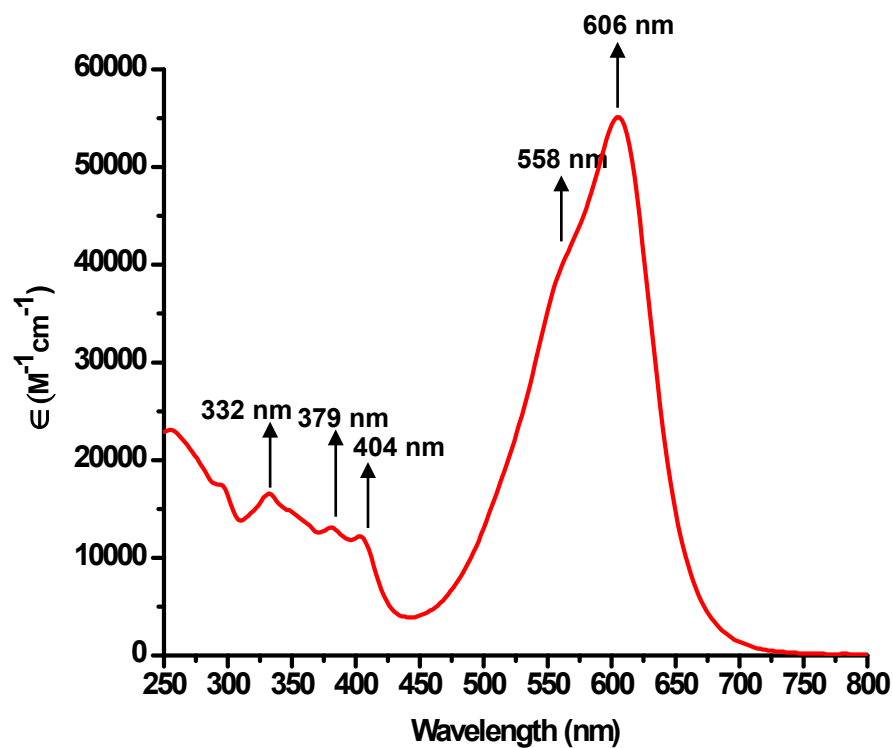


Figure S2. UV-visible spectra of dyad **5a** in dichloromethane and resolved peaks after band-fitting. (Black: experimental, Green: fitted curve)

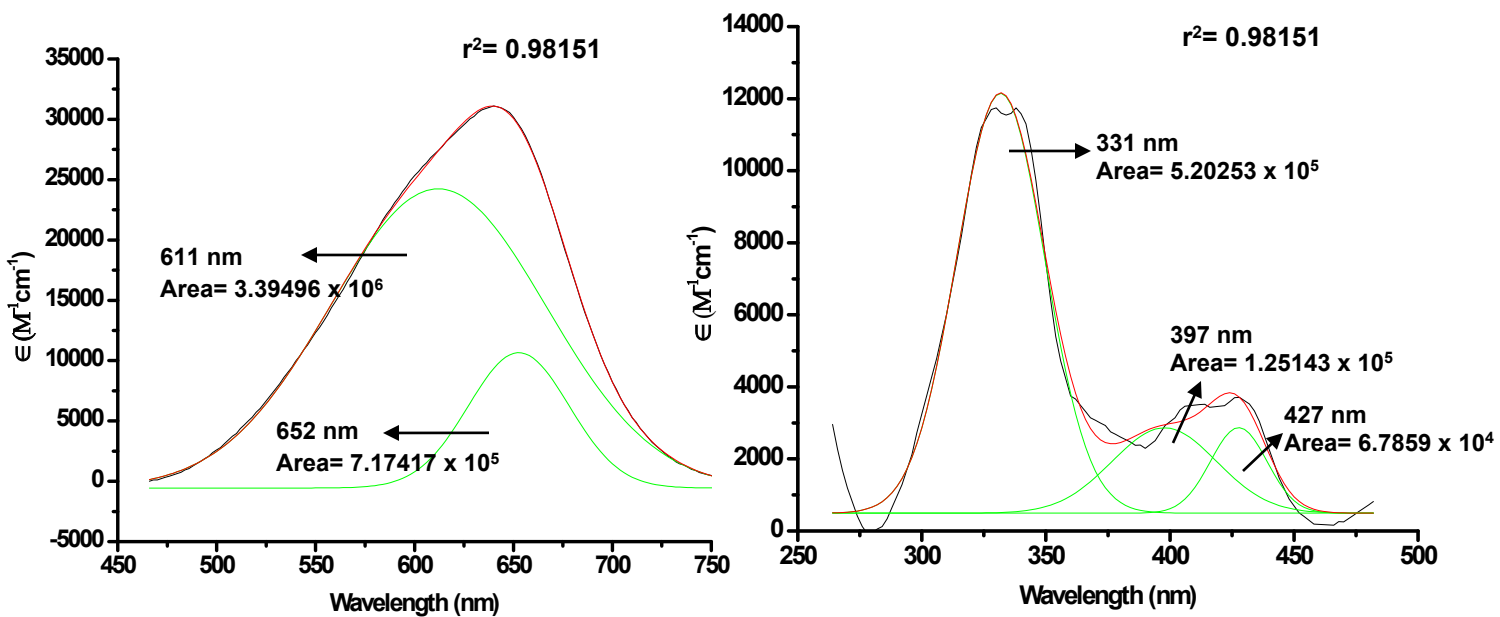
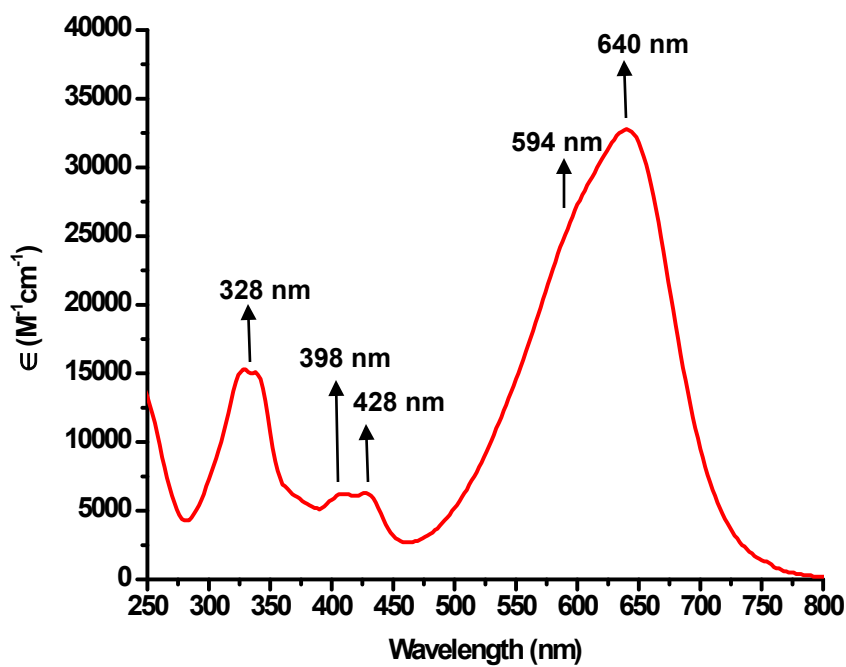


Figure S3. UV-visible spectra of dyad **5b** in dichloromethane and resolved peaks after band-fitting. (Black: experimental, Green: fitted curve)

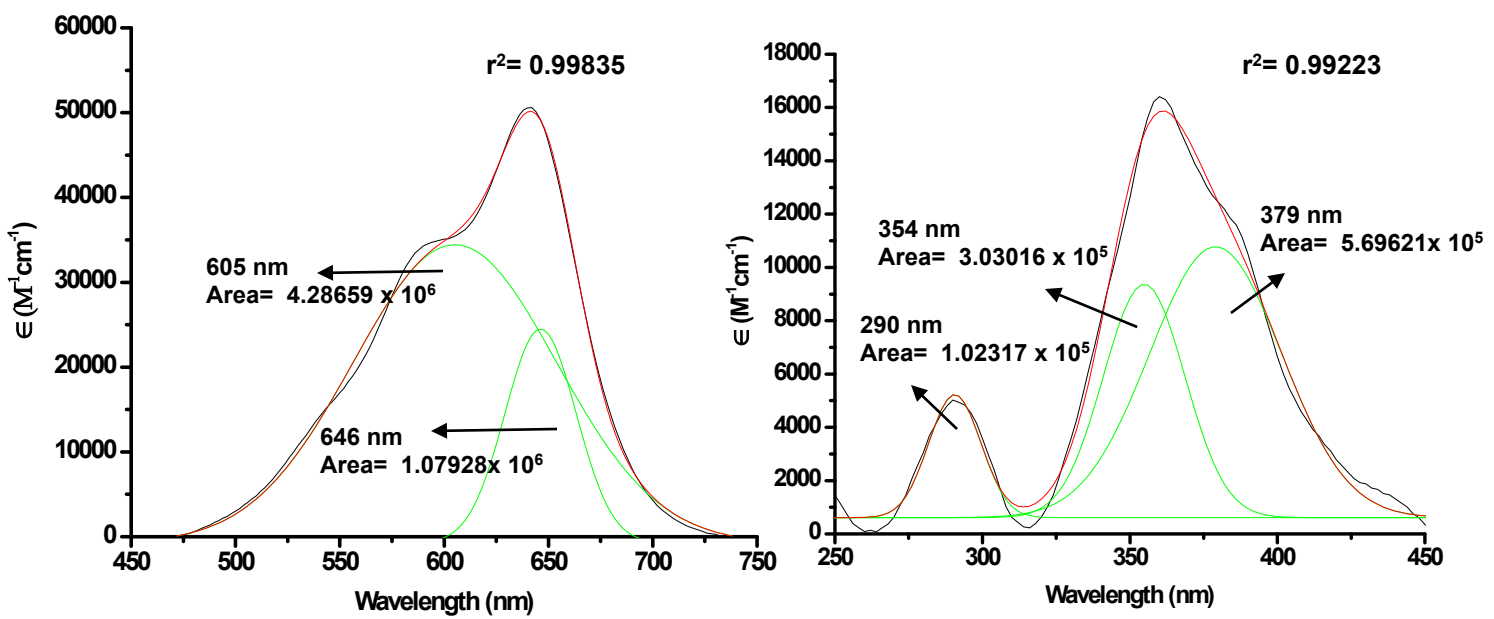
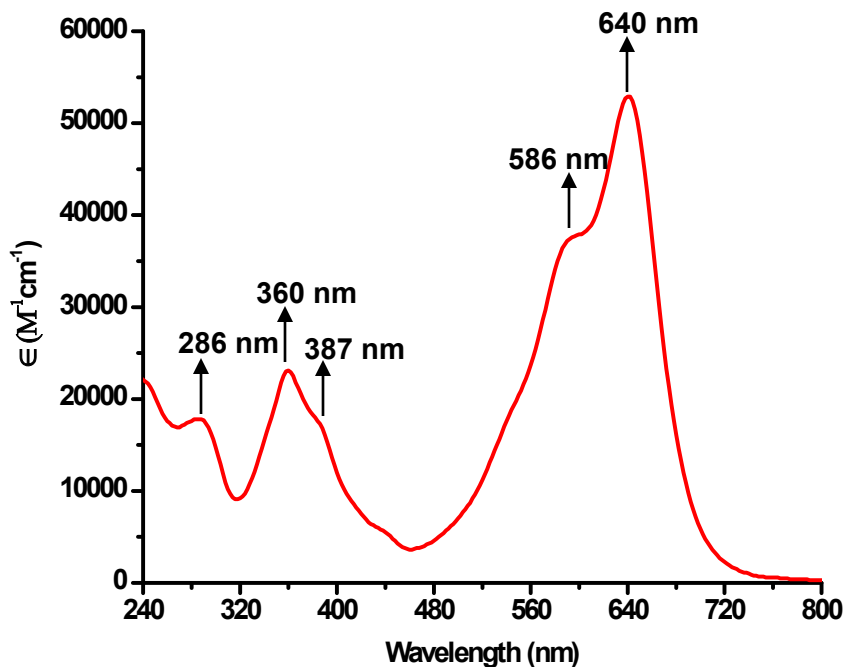


Figure S4. UV-visible spectra of dyad **5c** in dichloromethane and resolved peaks after band-fitting. (Black: experimental, Green: fitted curve)

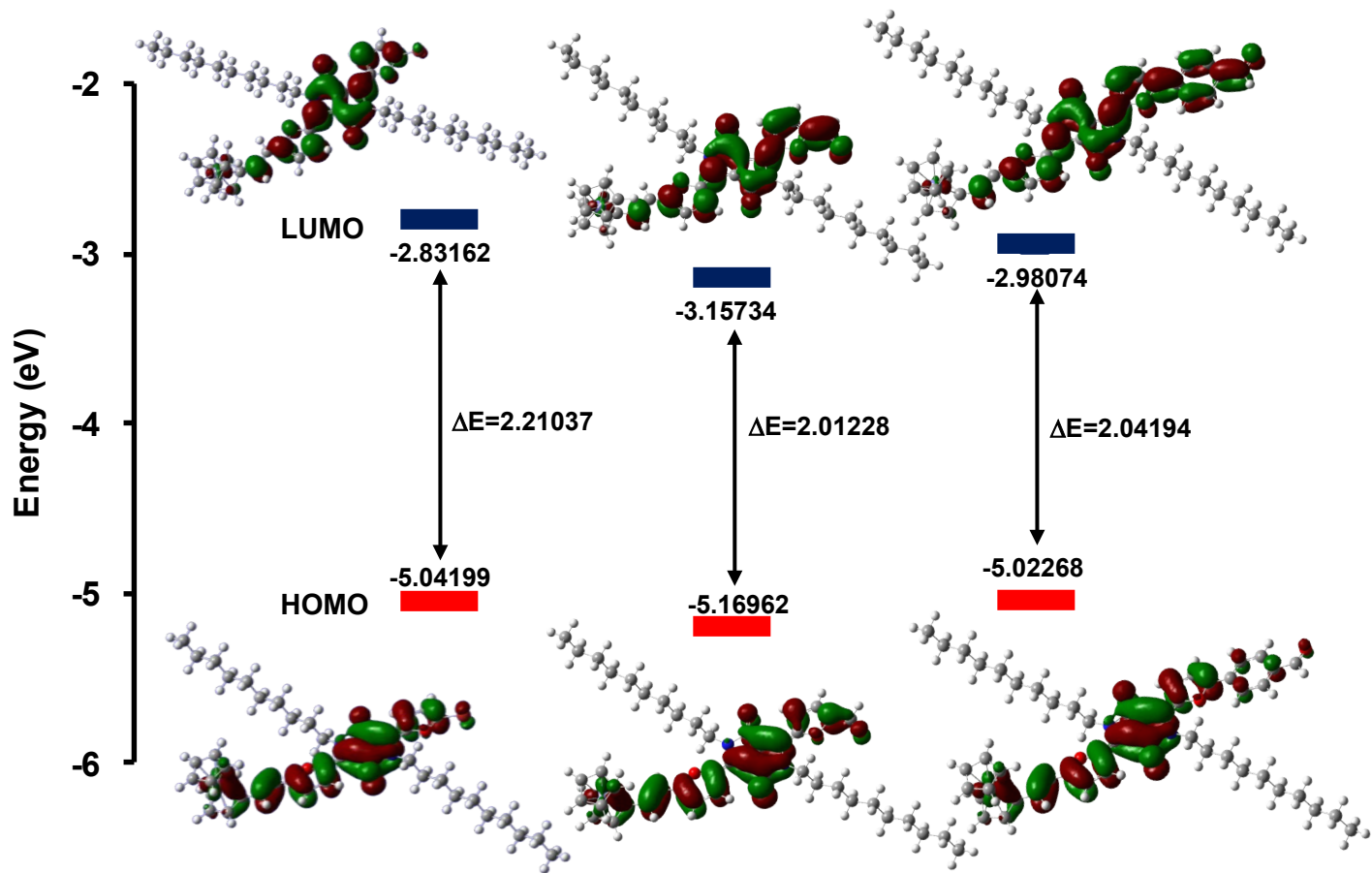


Figure S5. Contour surfaces of frontier molecular orbitals of dyads **5a-c** derived from TD-DFT at B3LYP/ 6-31G basis set (Iso-surface value= 0.02).

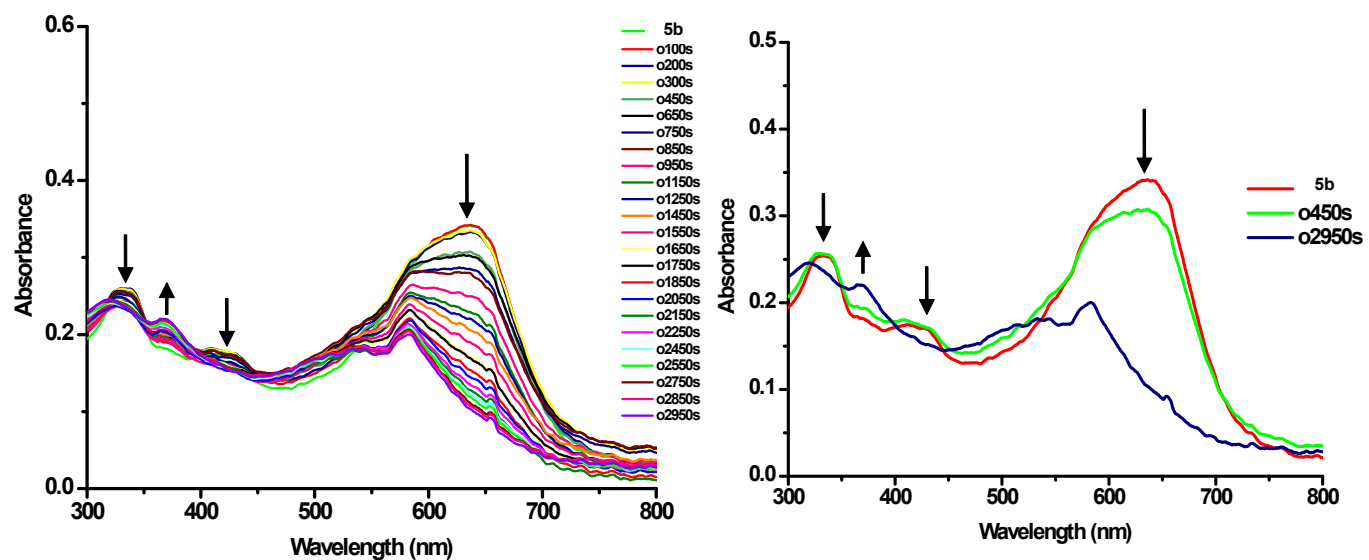


Figure S6. Spectro-electrochemical curve of chromophore **5b** recorded at 1×10^{-5} M in dichloromethane

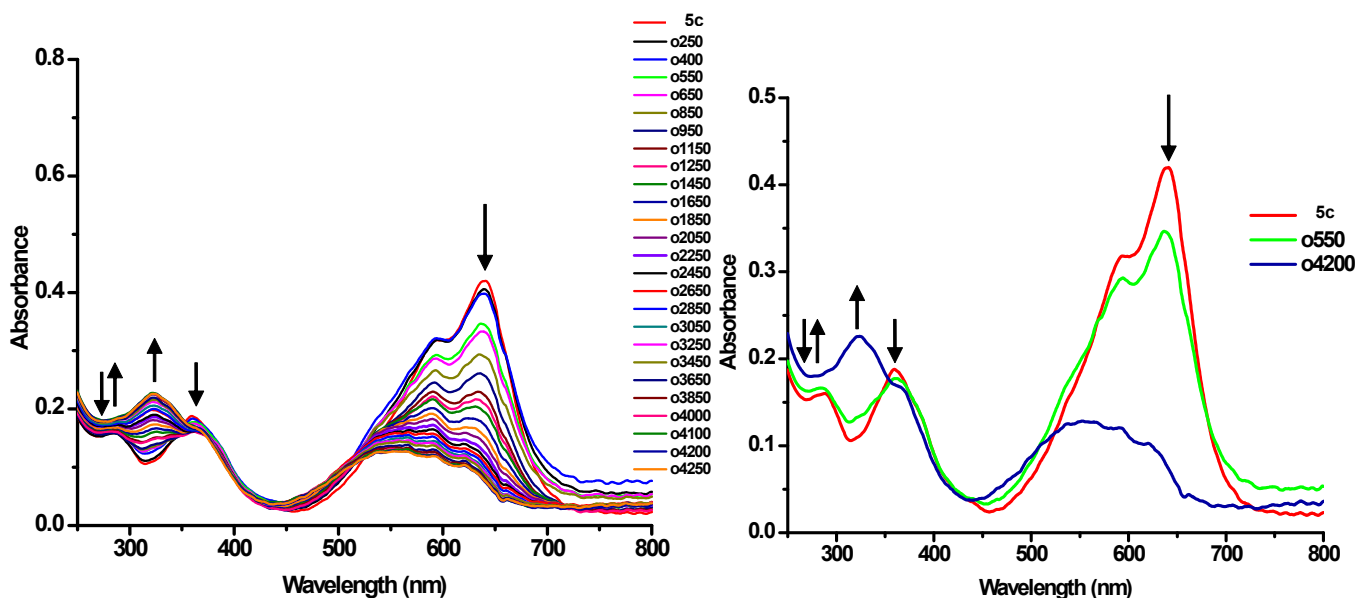


Figure S7. Spectro-electrochemical curve of chromophore **5c** recorded at 1×10^{-5} M in dichloromethane.

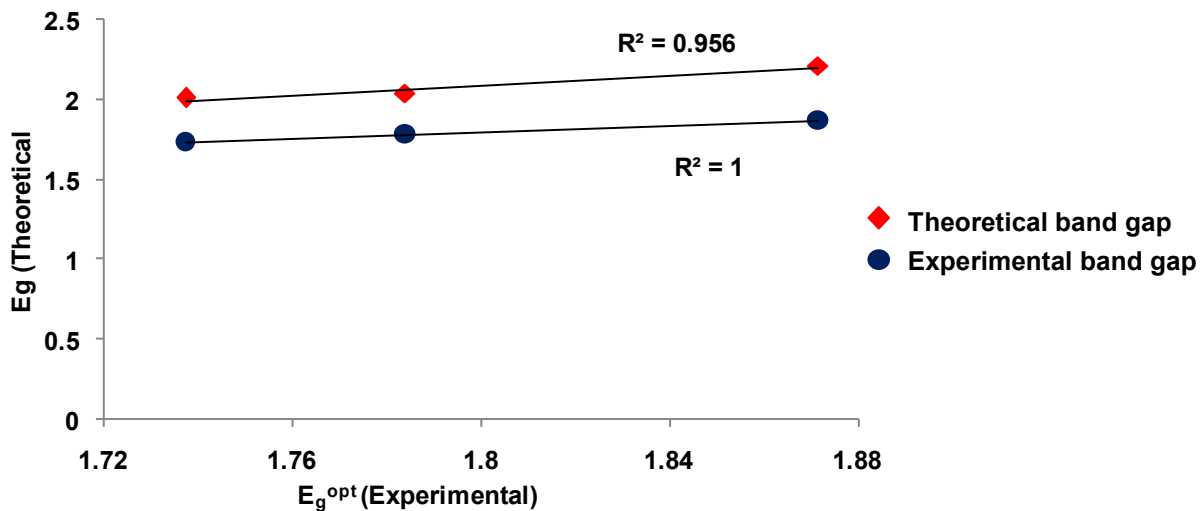


Figure S8. Linear correlation between the optical gap E_g^{opt} , determined from UV/CV and TD-DFT for the dyads **5a-c**.

Table S2. Energies of the Frontier Orbitals (eV) HOMO-n to LUMO+n (n=0-6) obtained from TD-DFT carried out at B3LYP/6-31G level in dichloromethane as solvent medium.

Dyads	5a	5b	5c
HOMO-6	-6.86815	-7.03795	-6.80176
HOMO-5	-6.77944	-6.87523	-6.52583
HOMO-4	-6.49373	-6.53617	-6.50270
HOMO-3	-6.11249	-6.19277	-6.10624
HOMO-2	-5.55548	-5.59793	-5.56554
HOMO-1	-5.52527	-5.58514	-5.52609
HOMO	-5.04199	-5.16962	-5.02268
LUMO	-2.83162	-3.15734	-2.98074
LUMO+1	-1.54289	-2.01854	-2.15378
LUMO+2	-0.77961	-1.32982	-1.45527
LUMO+3	-0.41959	-0.60001	-0.75131
LUMO+4	-0.30640	-0.34667	-0.48028
LUMO+5	-0.15075	-0.16926	-0.31674
LUMO+6	0.24681	0.65661	-0.17715

Table S3. Energies of the Frontier Orbitals (eV) HOMO-n to LUMO+n (n=0-6) obtained from TD-DFT carried out at B3LYP/6-31G level in gas phase.

Dyads	5a	5b	5c
HOMO-6	-6.72203	-7.02544	-6.69101
HOMO-5	-6.59604	-6.73781	-6.62352
HOMO-4	-6.57237	-6.68747	-6.44202
HOMO-3	-6.06623	-6.21943	-6.12093
HOMO-2	-5.63330	-5.74813	-5.68419
HOMO-1	-5.55847	-5.68527	-5.60718
HOMO	-4.88417	-5.08635	-4.92853
LUMO	-2.66182	-3.04387	-2.88359
LUMO+1	-1.47186	-1.95296	-2.08031
LUMO+2	-0.66505	-1.31268	-1.43214
LUMO+3	-0.38858	-0.54967	-0.68763
LUMO+4	-0.38586	-0.49797	-0.51619
LUMO+5	-0.19429	-0.26613	-0.43702
LUMO+6	0.37906	0.76355	-0.25524

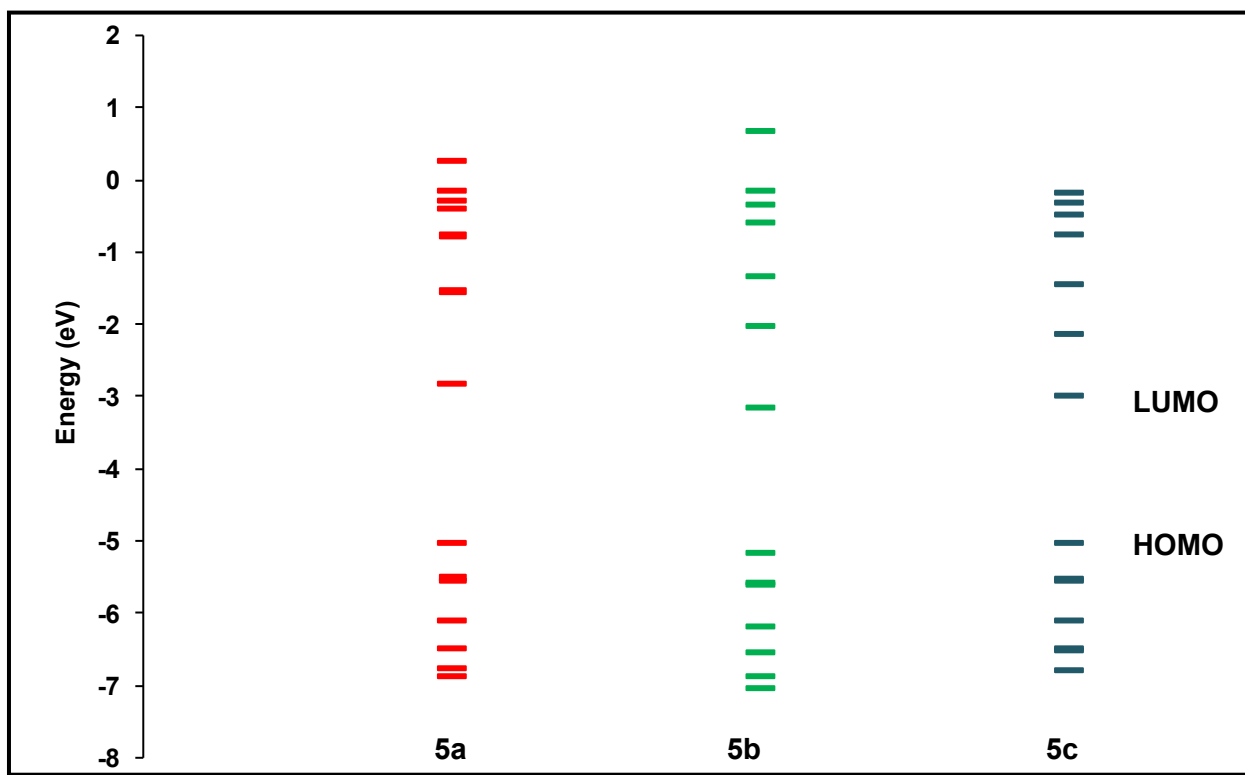


Figure S9. B3LYP/6-31G predicted orbital energy level diagram for the dyads **5a-c**.

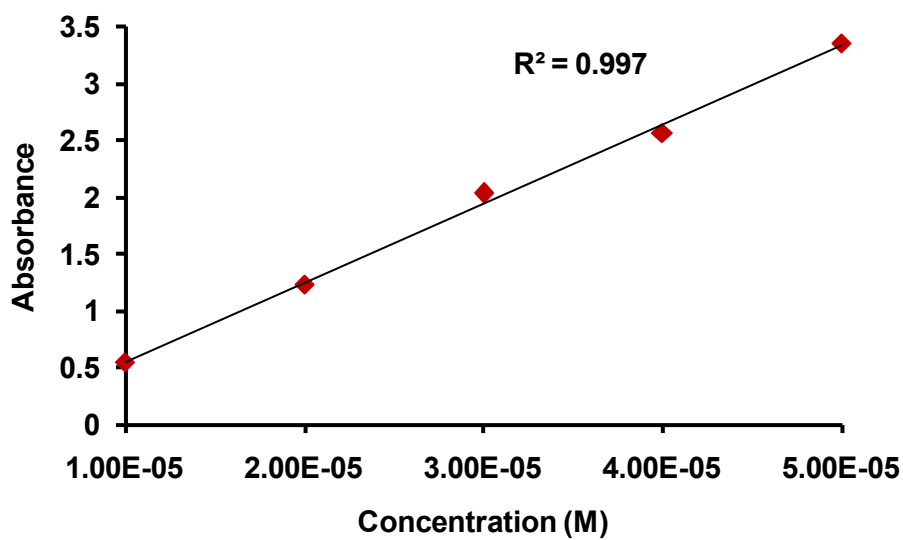


Figure S10. Linear correlation of absorbance and concentration of **5a** at 606 nm.

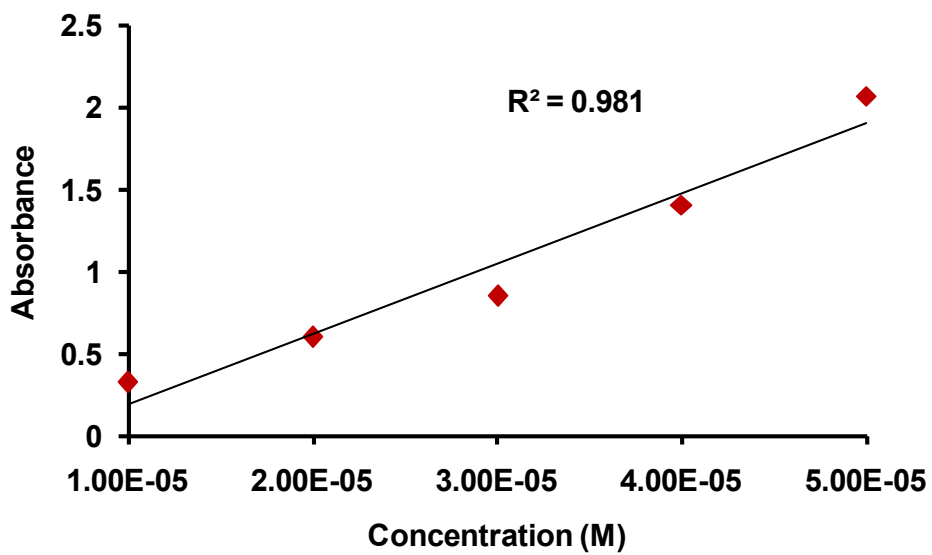


Figure S11. Linear correlation of absorbance and concentration of **5b** at 640 nm.

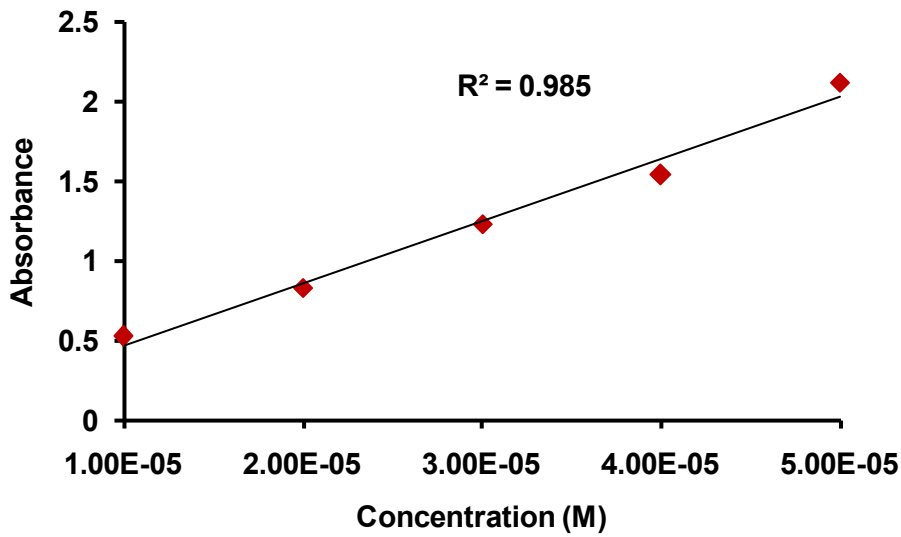


Figure S12. Linear correlation of absorbance and concentration of **5c** at 640 nm.

Table S4. Comparison of experimentally (UV-visible) and theoretically (TD-DFT) calculated absorption bands and assignment of electronic transitions for the dyads **5a-c**.

Dyad	$\lambda_{\text{exp}}^{\text{a}}$ (nm)	E(eV)/ $\lambda_{\text{theor}}^{\text{b}}$ (nm)	Oscillator strength, <i>f</i>	Transition	Assignment	CI coefficient
5a	606	2.1270/ 553.75	0.8644	3A H-2->L+4	M→Cp ring	-0.24844 (12%)
				H->L	D→A+ $\pi\rightarrow\pi^*$	0.55219 (61%)
	558	2.3590/ 499.29	0.0258	4A, H-4->L+5	M→Cp ring	-0.29834 (18%)
				H-2->L+4	M→Cp ring	0.43672 (43%)
				H-1->L	D→A	0.29406 (17%)
	404	2.8788/ 409.14	0.0648	8A, H-3->L	D→A+ $\pi\rightarrow\pi^*$	0.62014 (77%)
				H->L+1	$\pi\rightarrow\pi^*$	-0.26583 (14%)
	379	3.2398/ 363.55	0.2698	11A, H-5->L	ILCT	0.23272 (11%)
				H-3->L	D→A	0.21999 (10%)
				HOMO->L+1	$\pi\rightarrow\pi^*$	0.57160 (65%)
	332	3.6155/	0.0658	15A, H-6->L	ILCT+	0.58449

		325.77			$\pi \rightarrow \pi^*$	(68%)
				H->L+2	$\pi \rightarrow \pi^*$	-0.26570 (14%)
5b	640	1.7690/ 665.82	0.8508	1A, H-1->L	D->A	-0.24444 (12%)
				H->L	D->A+ $\pi \rightarrow \pi^*$	0.59009 (70%)
	594	2.0063/ 587.07	0.5200	3A, H-1->L	D->A	0.40514 (33%)
				H->L	D->A+ $\pi \rightarrow \pi^*$	0.39188 (31%)
	428	2.7085/ 434.86	0.0623	8A, H-3->L	D->A+ $\pi \rightarrow \pi^*$	0.63856 (82%)
				H->L+1	$\pi \rightarrow \pi^*+$ D->A	-0.23667 (11%)
	398	2.8860/ 408.12	0.2193	9A, H-3->L	$\pi \rightarrow \pi^*+$ D->A	0.23058 (11%)
				H->L+1	$\pi \rightarrow \pi^*$	0.57450 (66%)
	328	2.9698/ 396.60	0.026	10A, H-5->L	$\pi \rightarrow \pi^*+$ ILCT	0.62147 (77%)
5c	640	1.8031/ 653.23	1.2955	1A, H->L	D->A+ $\pi \rightarrow \pi^*$	0.62144 (77%)
	586	2.0091/ 586.25	0.4269	3A, H-2->L+5	M->Cp ring	-0.26282 (14%)
				H-1->L	D->A	0.34936 (24%)
				H-1->L+6	M->Cp ring + $\pi \rightarrow \pi^*$	-0.26444 (14%)
				H->L	D->A+ $\pi \rightarrow \pi^*$	0.33754 (23%)
	387	2.8152/ 418.38	0.1008	9A, H-3->L	D->A+ $\pi \rightarrow \pi^*$	0.63774 (81%)
	360	3.2008/ 367.98	0.2125	14A, H-5->L	ILCT	0.50406 (51%)
				H-4->L	D->A	-0.26176 (14%)
				H-1->L+1	D->A	0.29802 (18%)
	286	3.6670/ 321.20	0.1706	20A, H-3->L+1	D->A+ $\pi \rightarrow \pi^*$	0.67267 (90%)

^aRecorded at 1x 10⁻⁵ M in dichloromethane. ^bCalculated from TD-DFT using B3LYP/6-31G and applying correction factor of 0.95. M: Metal. D- Donor. A-Acceptor.

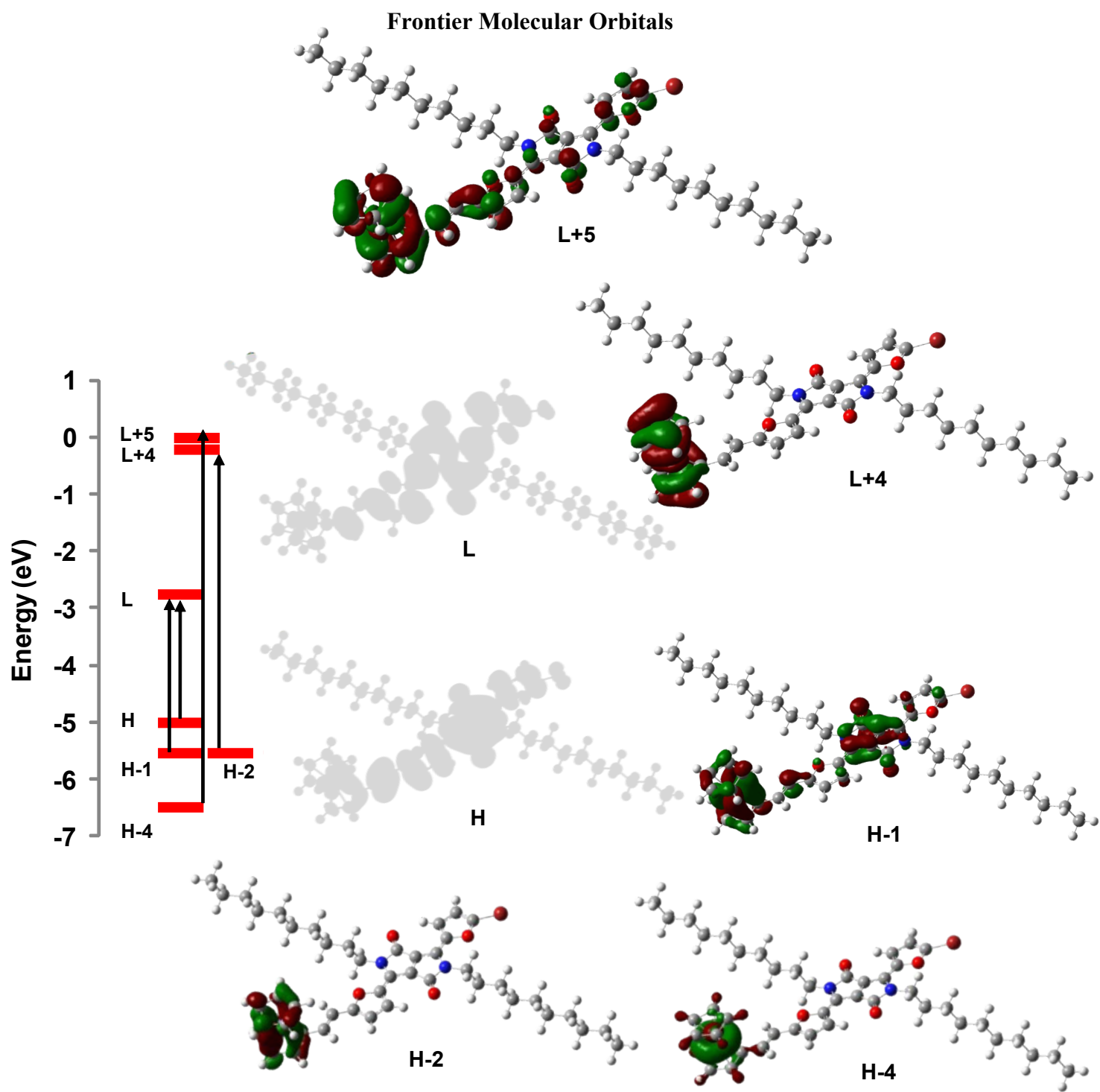


Figure S13. Contour surfaces of frontier molecular orbitals involved in LE electronic transitions of the dyad **5a** obtained from TD-DFT calculations using dichloromethane as solvent at an iso-surface value of 0.02 au.

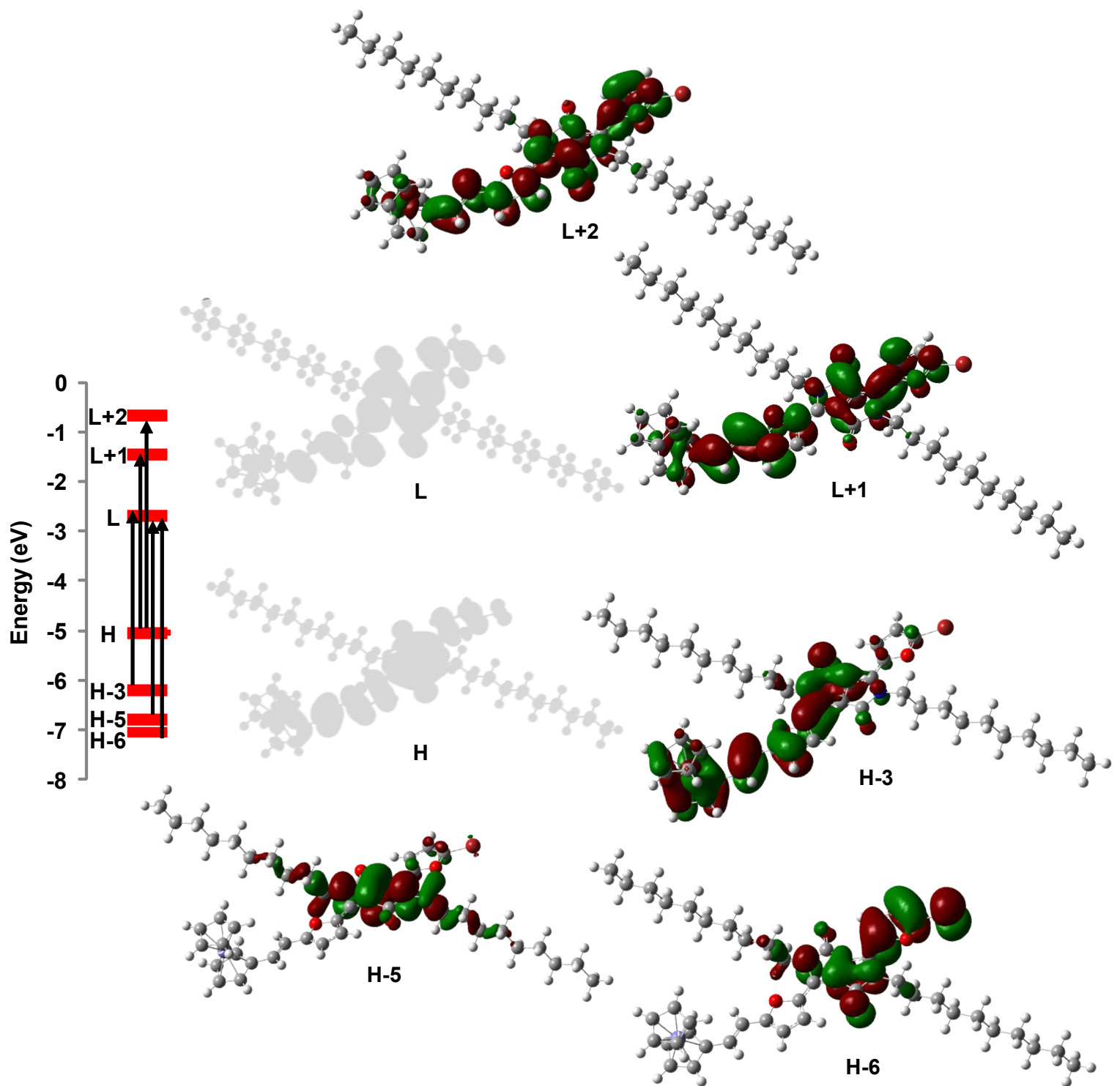


Figure S14. Contour surfaces of frontier molecular orbitals involved in HE electronic transitions of the dyad **5a** obtained from TD-DFT calculations using dichloromethane as solvent at an iso-surface value of 0.02 au.

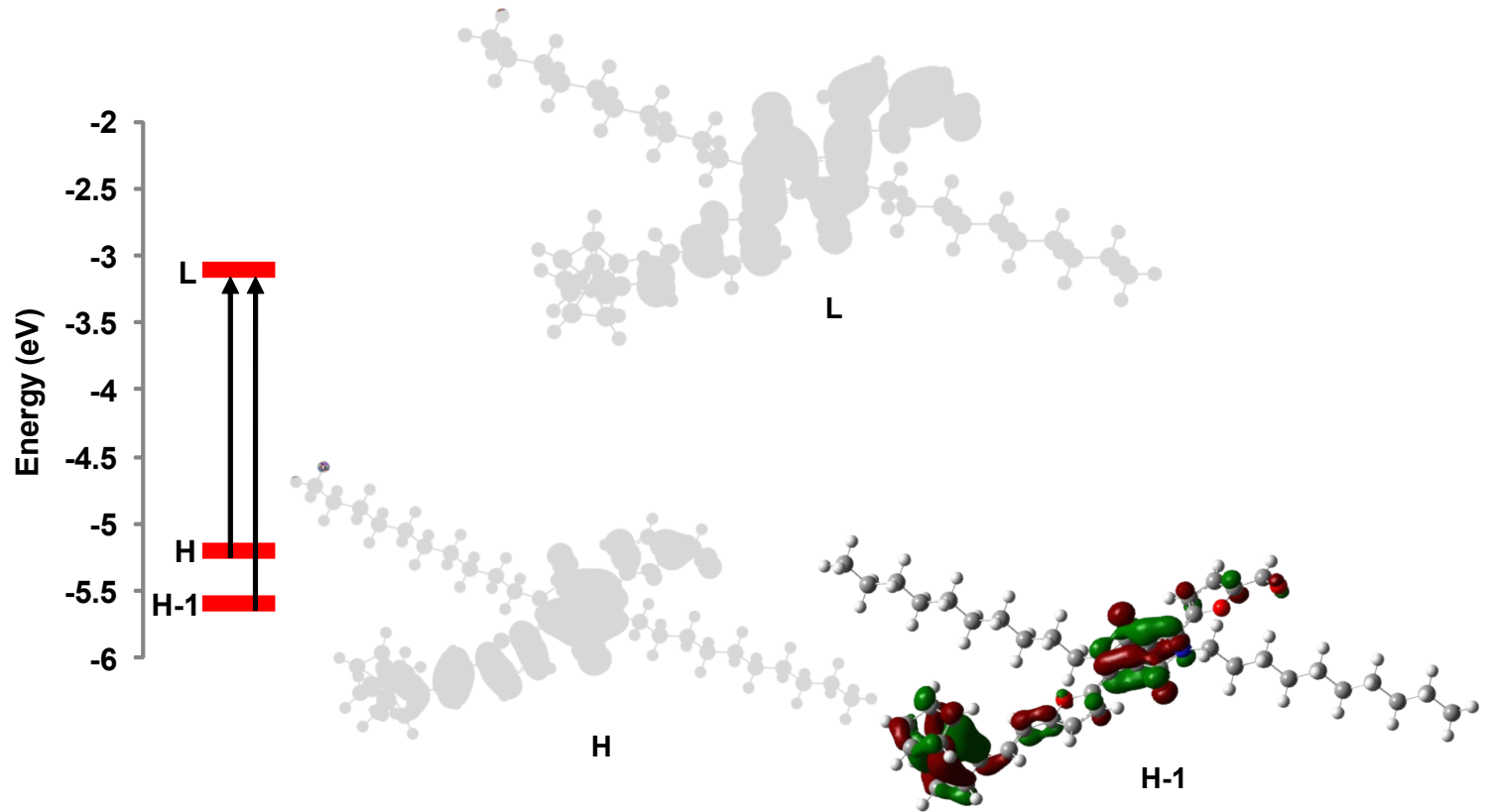


Figure S15. Contour surfaces of frontier molecular orbitals involved in LE electronic transitions of the dyad **5b** obtained from TD-DFT calculations using dichloromethane as solvent at an iso-surface value of 0.02 au.

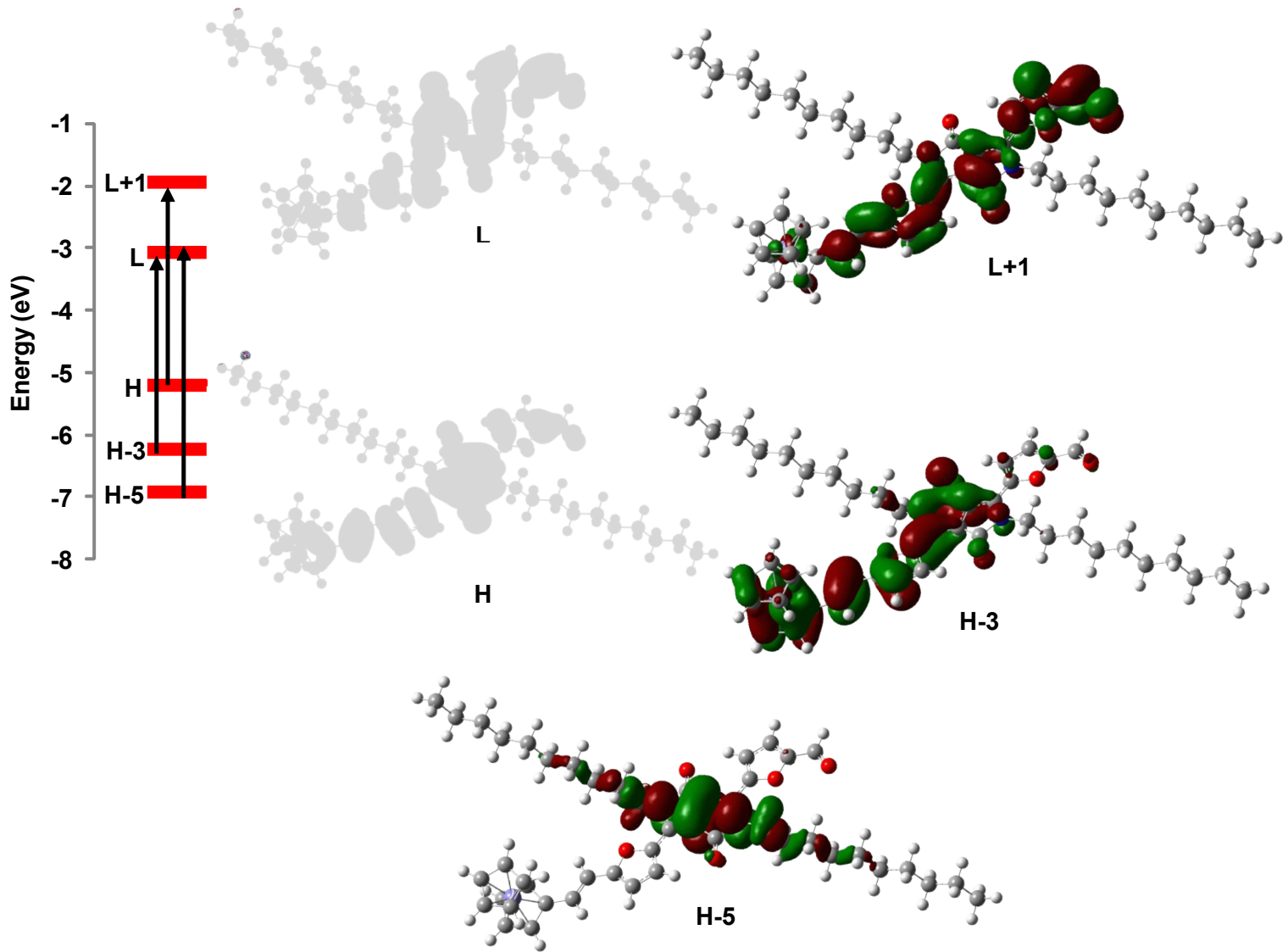


Figure S16. Contour surfaces of frontier molecular orbitals involved in HE electronic transitions of the dyad **5b** obtained from TD-DFT calculations using dichloromethane as solvent at an iso-surface value of 0.02 au.

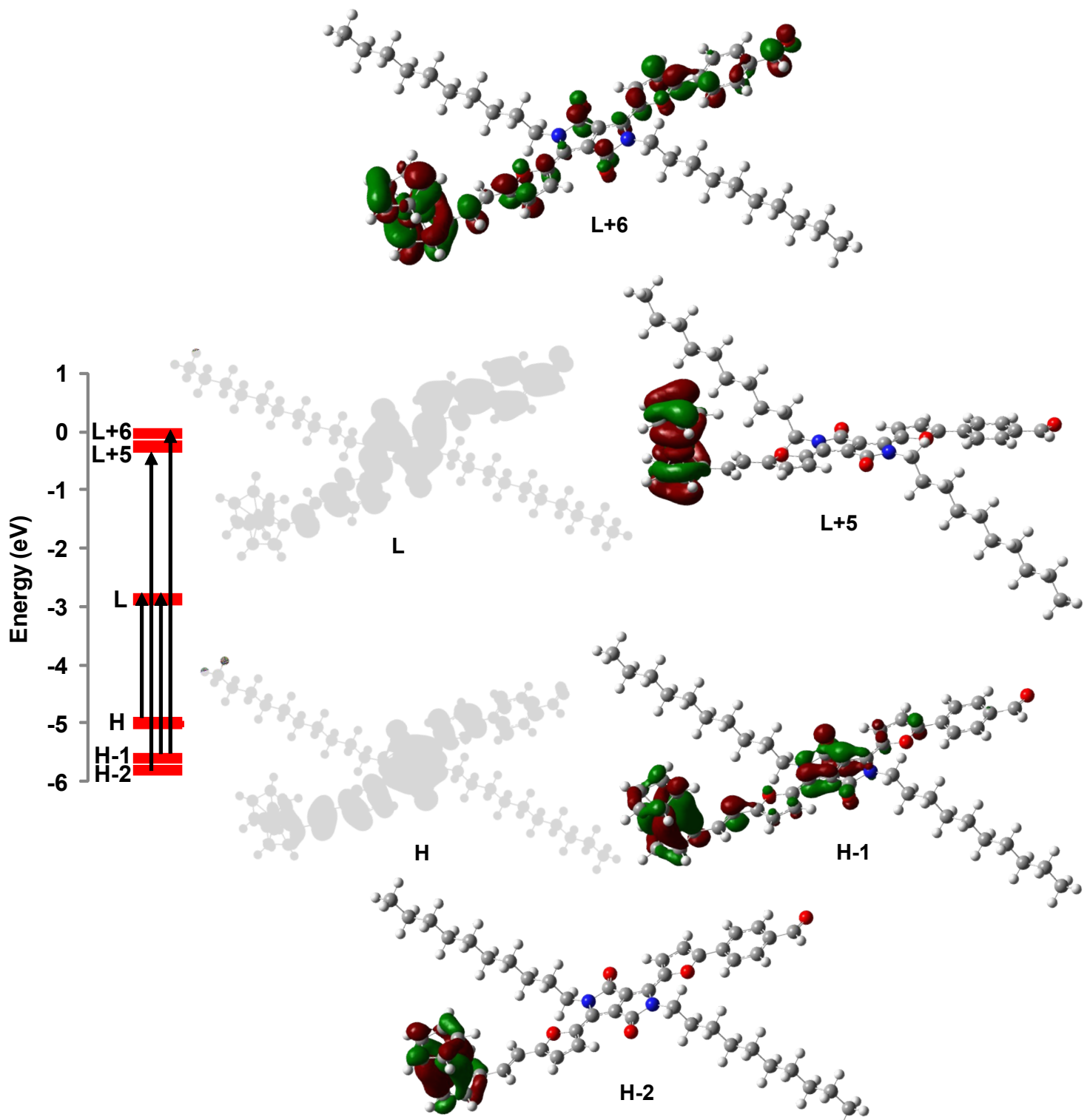


Figure S17. Contour surfaces of frontier molecular orbitals involved in LE electronic transitions of the dyad **5c** obtained from TD-DFT calculations using dichloromethane as solvent at an iso-surface value of 0.02 au.

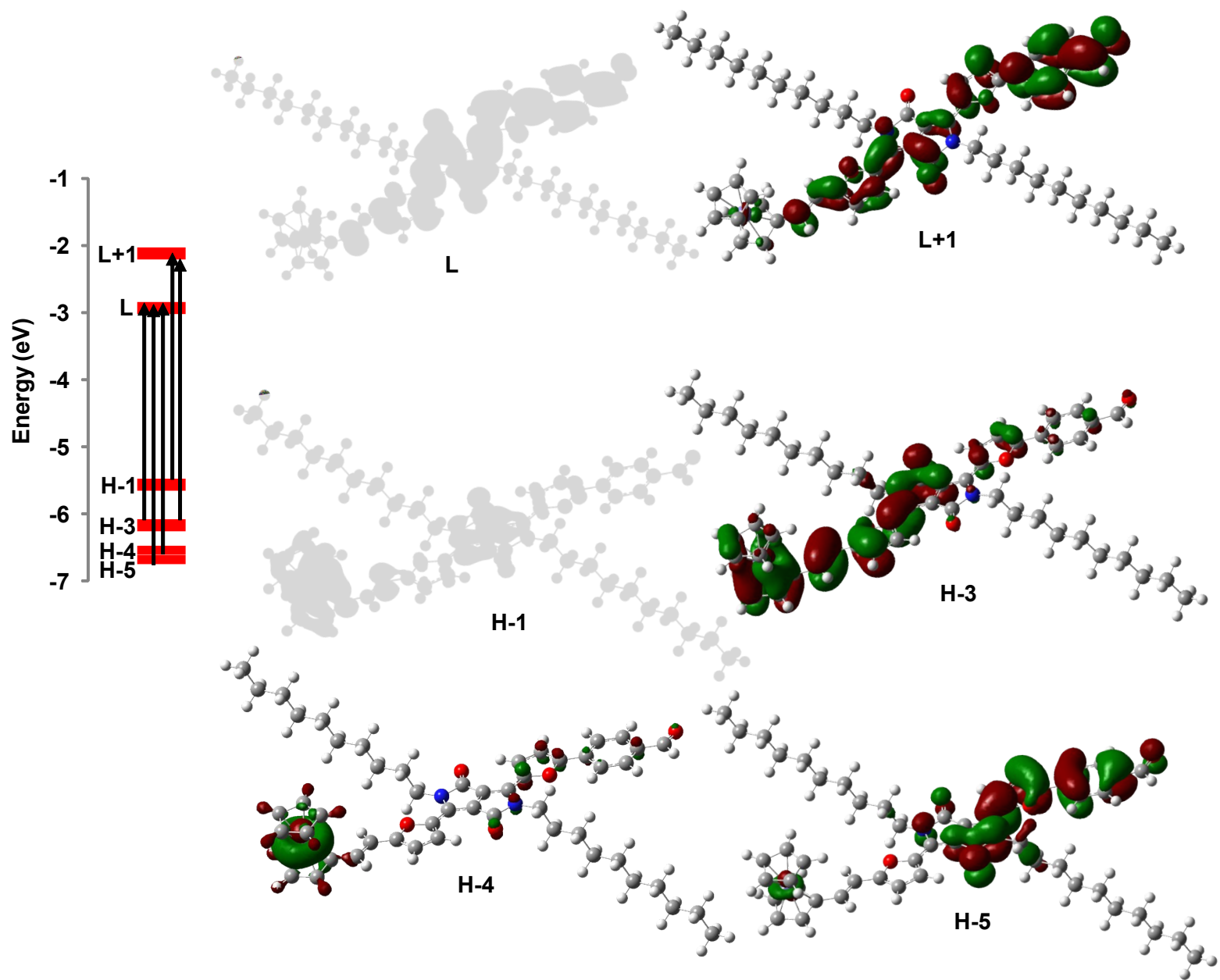


Figure S18. Contour surfaces of frontier molecular orbitals involved in HE electronic transitions of the dyad **5c** obtained from TD-DFT calculations using dichloromethane as solvent at an iso-surface value of 0.02 au.

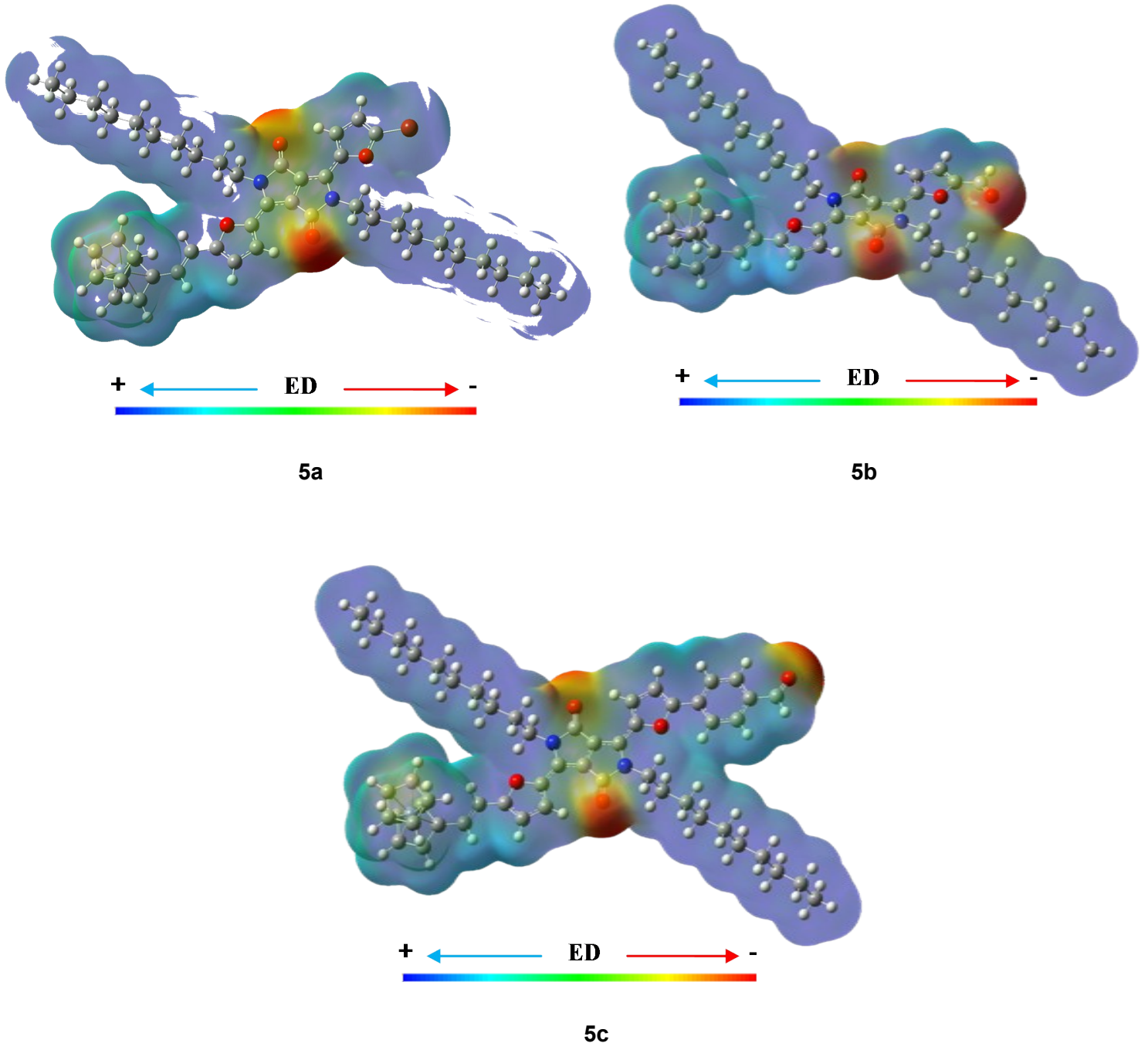


Figure S19. Electron density maps of dyads **5a-c** with iso-value of 0.0004.

Table S5. UV-visible data of **5a-c** in various solvents.^a

Solvent	Hexane	Toluene	Diethyl ether	DCM	THF	Methanol	ACN	DMF	DMSO
Dyad									
5a	593 (71074)	605 (60398)	594 (67031)	606 (55100)	601 (53300)	597	597 (61766)	606 (55278)	610 (44077)
	549 (50443)	557 (41248)	550 (47261)	558 (38800)	553 (37664)	552	552 (44660)	559 (41587)	563 (34173)
	400 (20160)	402 (12974)	400 (10010)	404 (12200)	403 (15993)	403	401 (12508)	403 (14791)	402 (6709)
	376 (21322)	380 (13842)	378 (10908)	379 (13100)	378 (16662)	378	382 (12678)	381 (14837)	382 (6946)
	329 (23668)	332 (16055)	329 (13797)	332 (16600)	330 (19999)	329	330 (16704)	332 (18349)	333 (11310)
5b	628 (40292)	639 (37460)	622 (46430)	640 (32800)	634 (36478)	610 (23197)	628 (30813)	627 (20909)	634
	566 (24546)	591 (27697)	--	594 (26000)	588 (28278)	--	--	--	--
	421 (3996)	425 (7473)	418 (11053)	428 (6300)	423 (6009)	--	424 (4364)	420 (2755)	--
	400 (4337)	406 (7609)	401 (11323)	398 (5700)	405 (6312)	405 (4013)	403 (4186)	408 (2524)	406
	335 (11978)	339 (14073)	332 (21227)	328 (15300)	327 (13783)	327 (8976)	324 (11110)	327 (7222)	337
5c	630 (30663)	642 (52359)	629 (67650)	640 (52900)	634 (51124)	nd	630	638 (39893)	632
	581 (19897)	591 (36522)	574 (46183)	586 (36400)	591 (37422)	nd	592	588 (30737)	595
	385 (5681)	388 (15263)	380 (18660)	387 (16800)	386 (15634)	nd	385	387 (14120)	--
	358 (9239)	362 (20005)	356 (24576)	360 (23100)	359 (21112)	nd	355	359 (18818)	359
	285 (5865)	289 (14999)	283 (17003)	286 (17800)	284 (15304)	nd	281	290 (14971)	--

^aAbsorption wavelength (nm) at room temperature ($c \approx 1 \times 10^{-5}$ M) and molar extinction coefficient between brackets ($M^{-1} \text{ cm}^{-1}$).

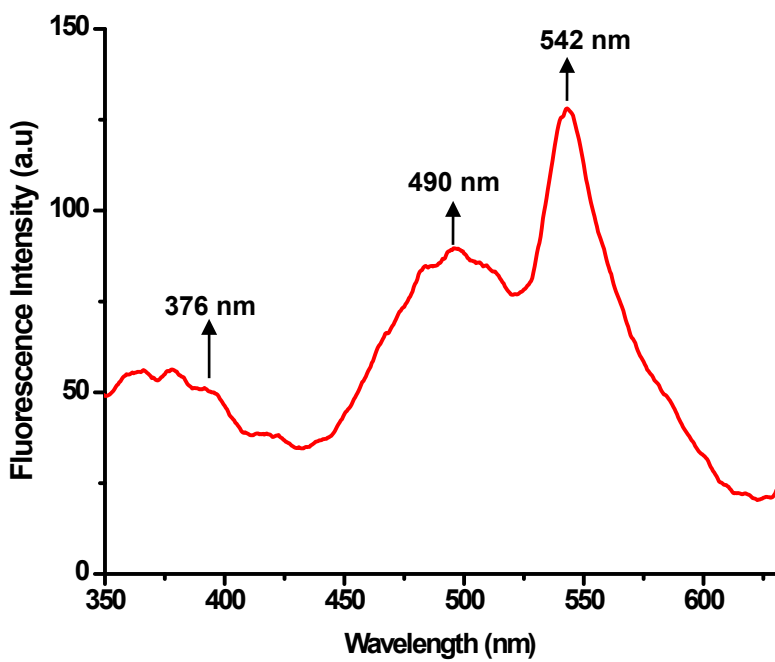


Figure S20. Emission spectra of **5a** at 1×10^{-5} in DCM at $\lambda_{\text{ex}} = 332$ nm.

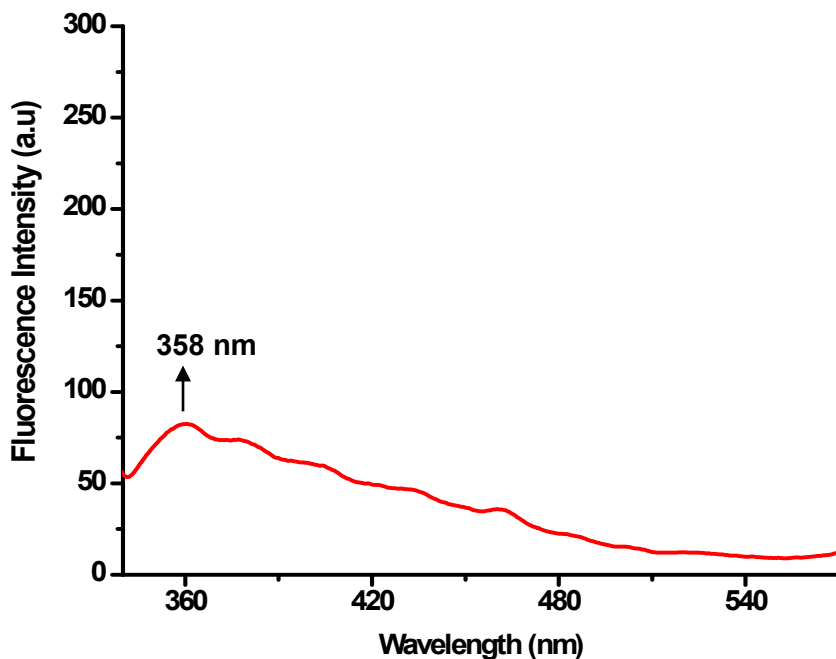


Figure S21. Emission spectra of **5b** at 1×10^{-5} in DCM at $\lambda_{\text{ex}} = 328$ nm.

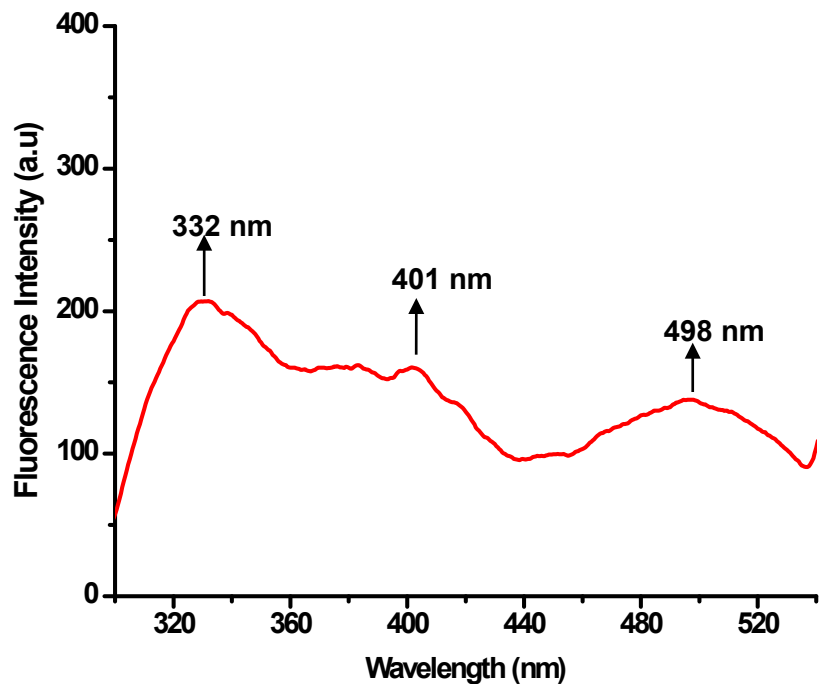


Figure 22a. Emission spectra of **5c** at 1×10^{-5} in DCM at $\lambda_{\text{ex}} = 286$ nm.

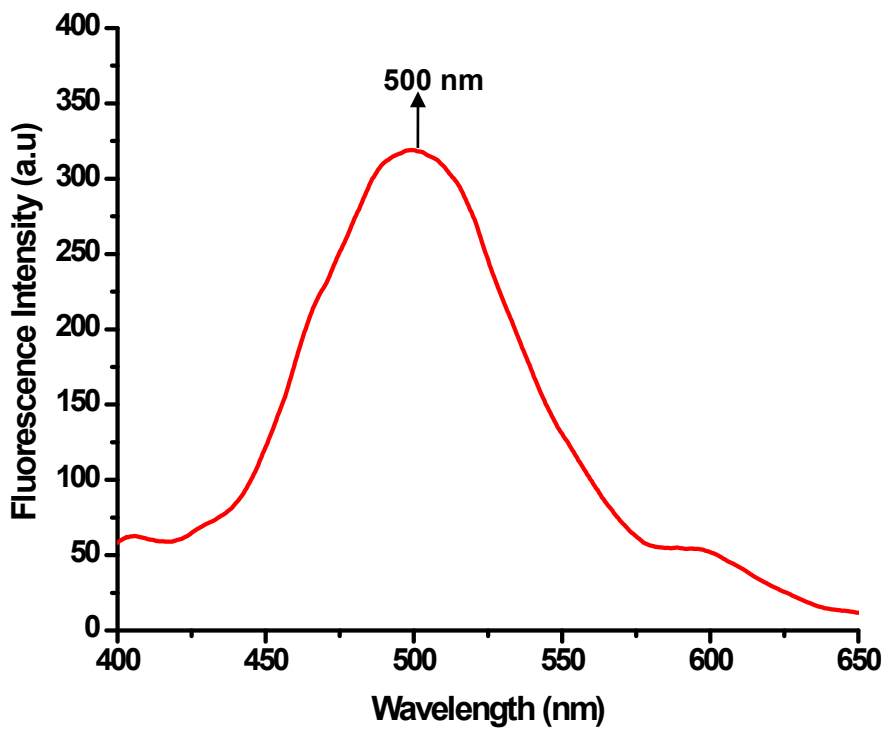


Figure 22b. Emission spectra of **5c** at 1×10^{-5} in DCM at $\lambda_{\text{ex}} = 360$ nm.

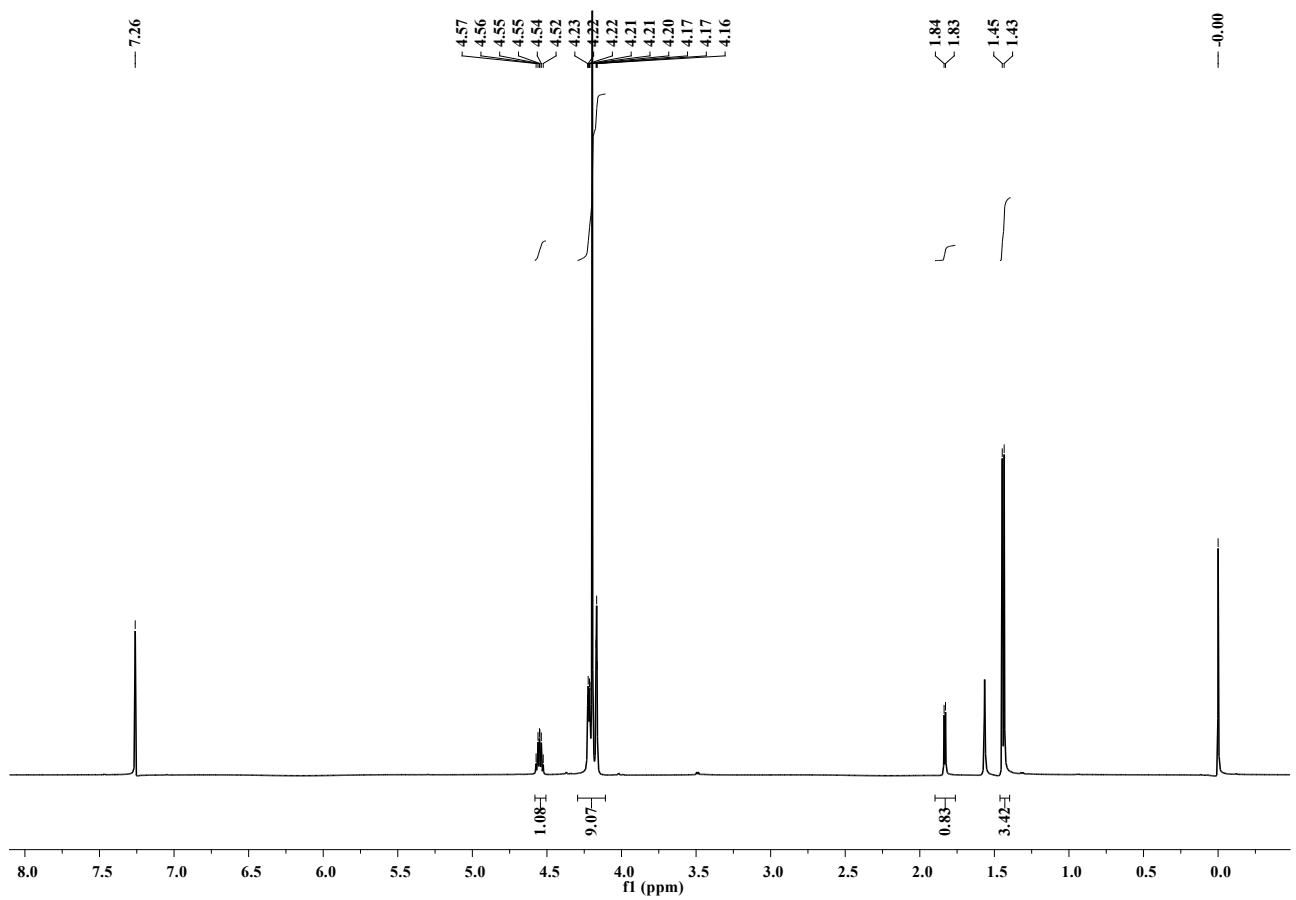


Figure S23. ${}^1\text{H}$ NMR of **2** (CDCl_3 , 500 MHz).

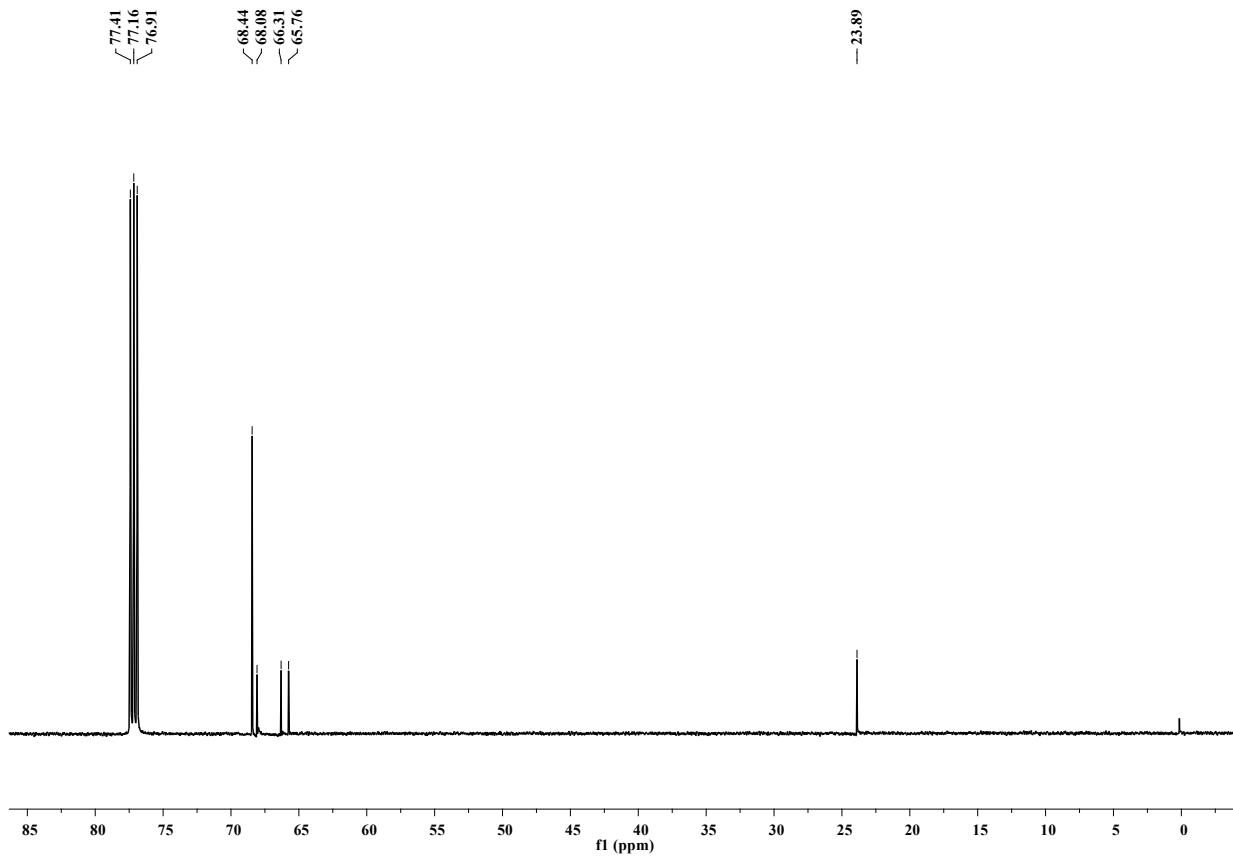


Figure S24. ^{13}C NMR of **2** (CDCl_3 , 500 MHz).

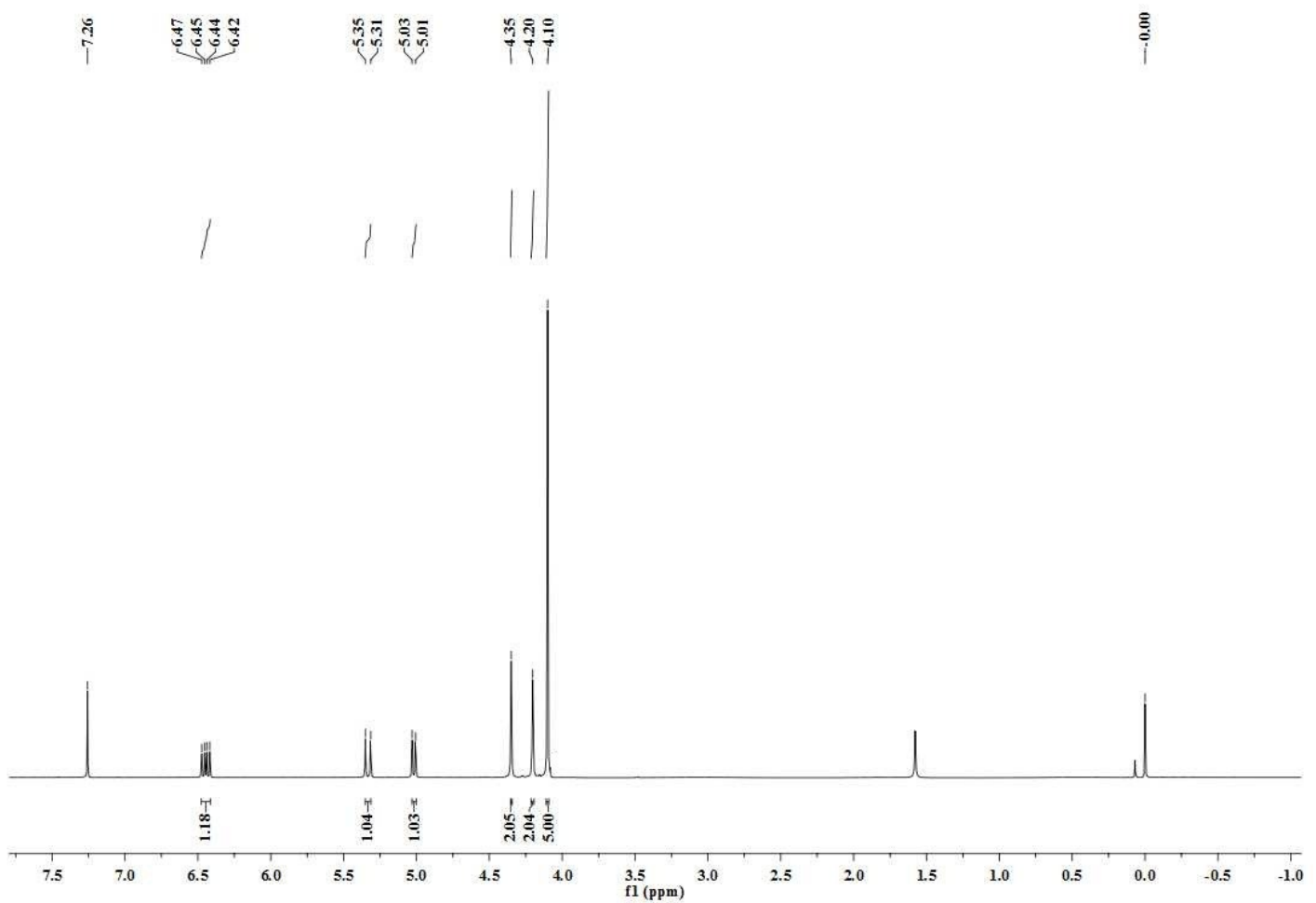


Figure S25. ${}^1\text{H}$ NMR of **3** (CDCl_3 , 500 MHz).

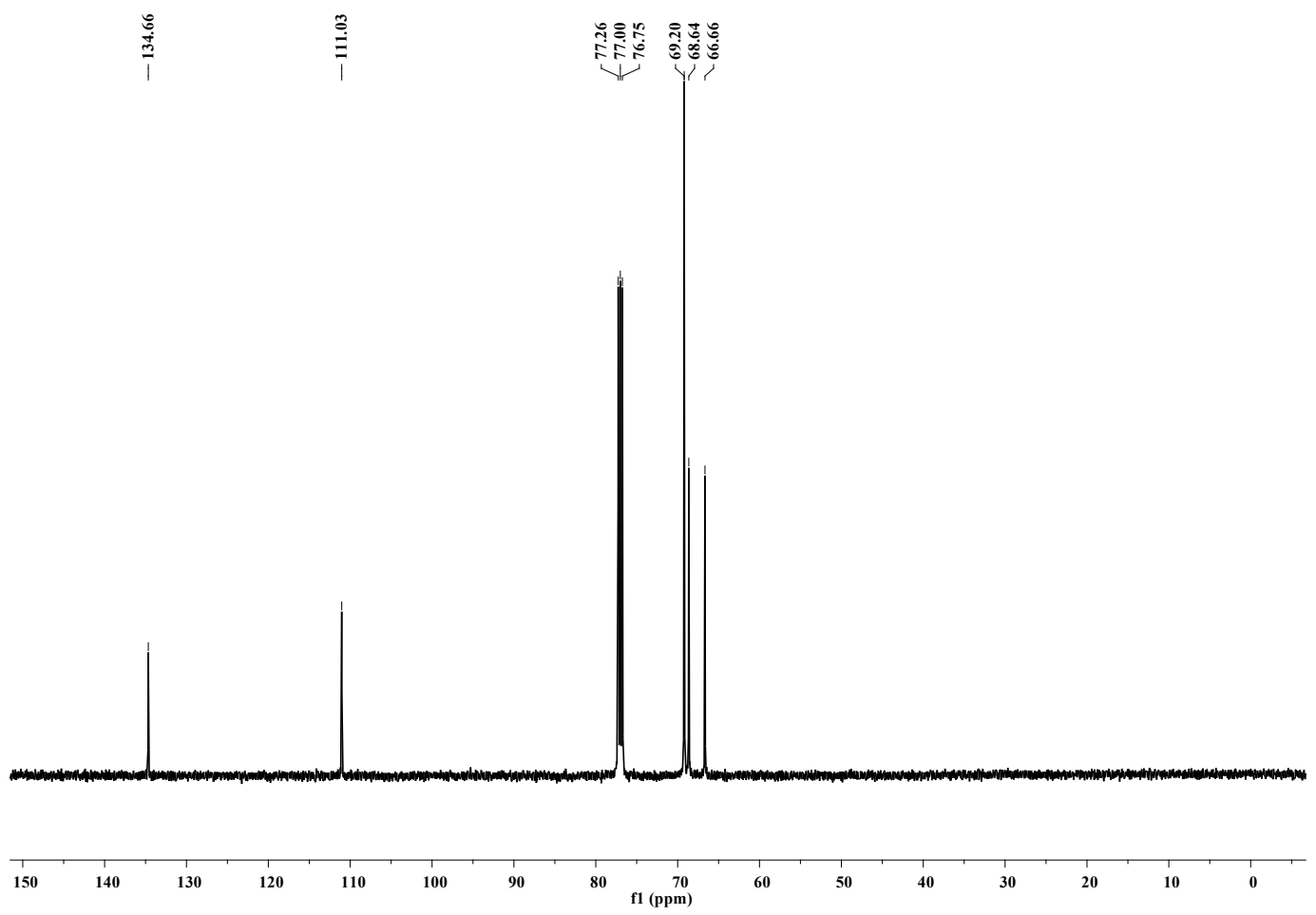


Figure S26. ^{13}C NMR of **3** (CDCl_3 , 500 MHz).

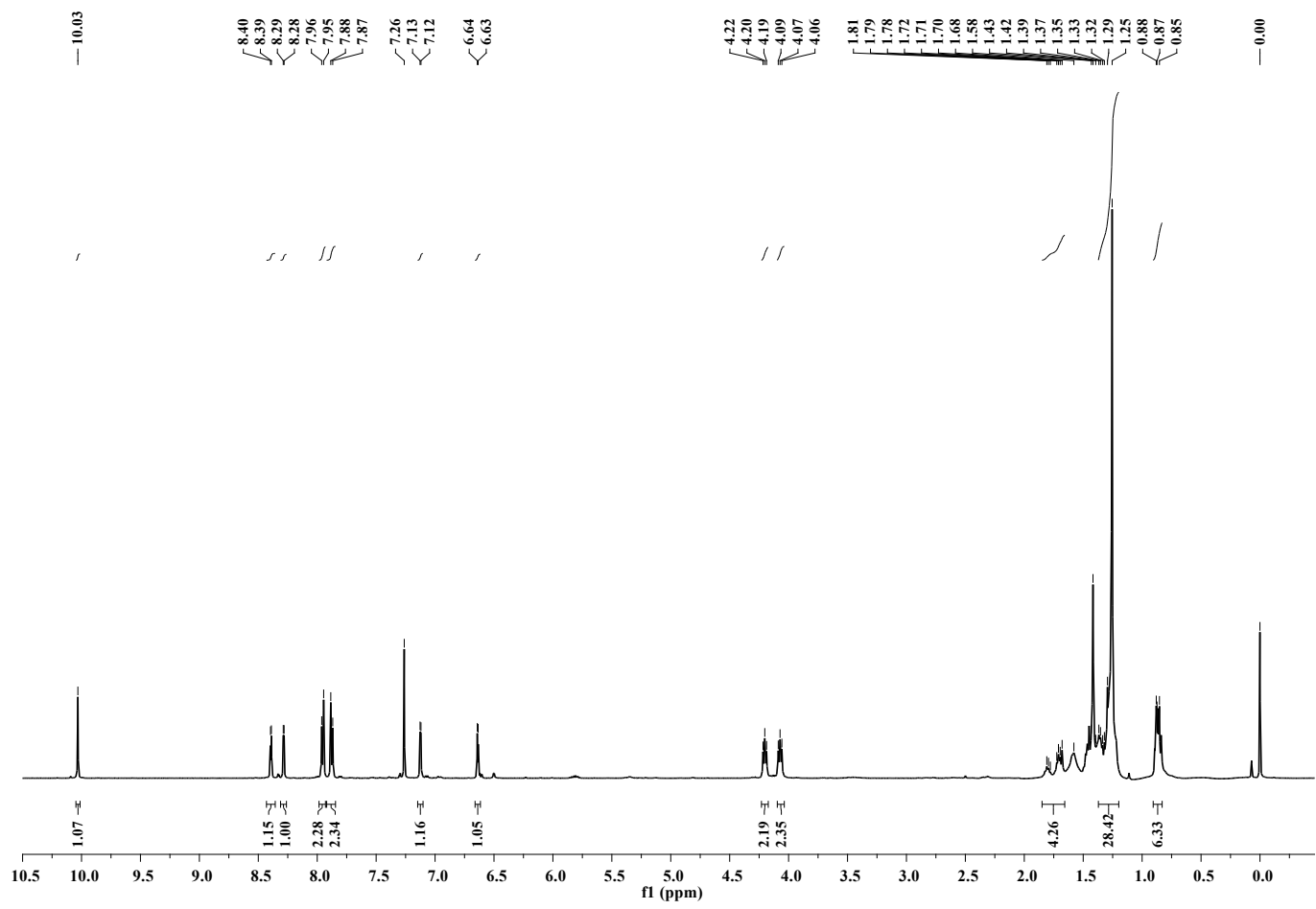


Figure S27. ^1H NMR of **7** (CDCl_3 , 500 MHz).

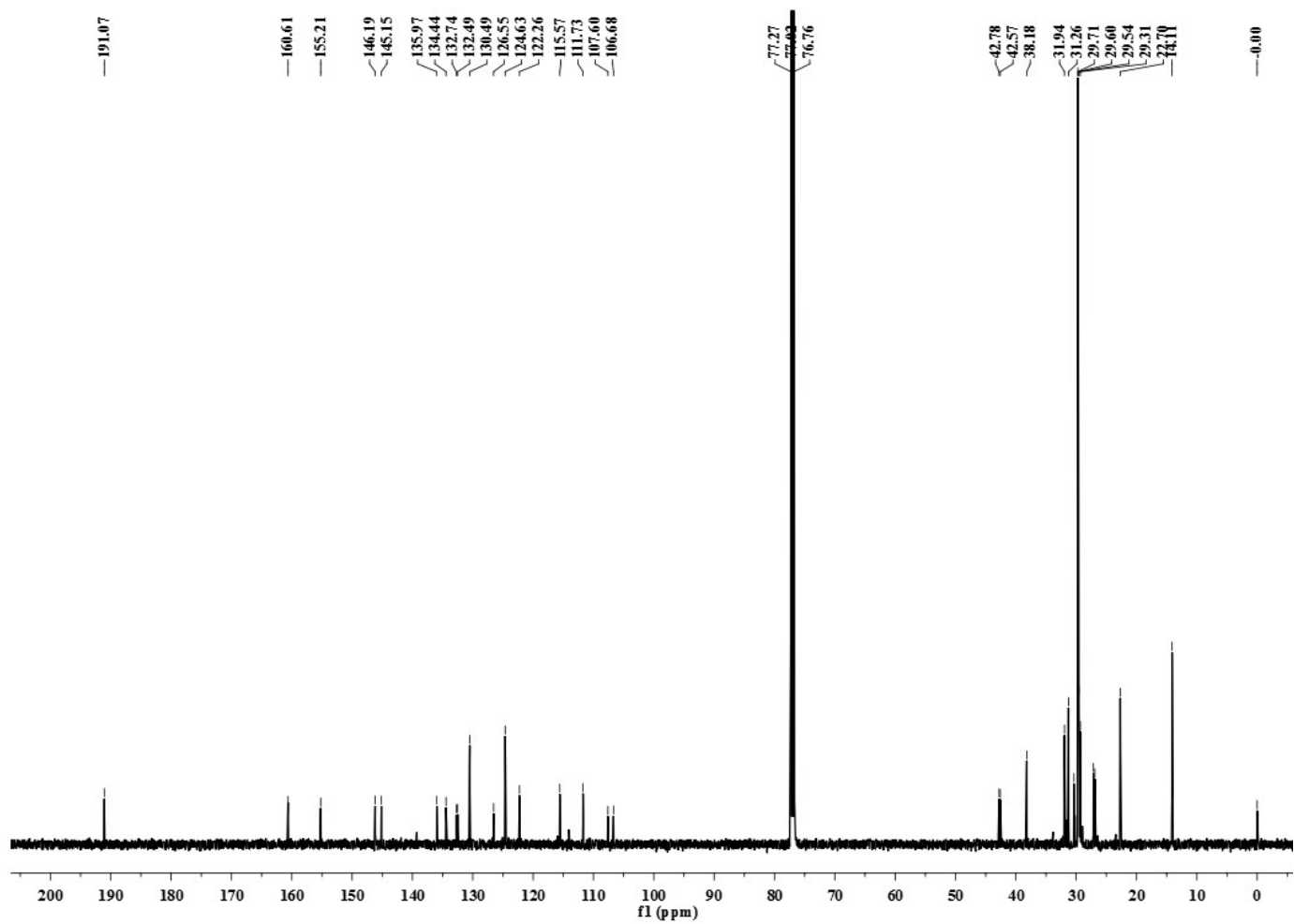


Figure S28. ${}^{13}\text{C}$ NMR of 7 (CDCl_3 , 500 MHz).

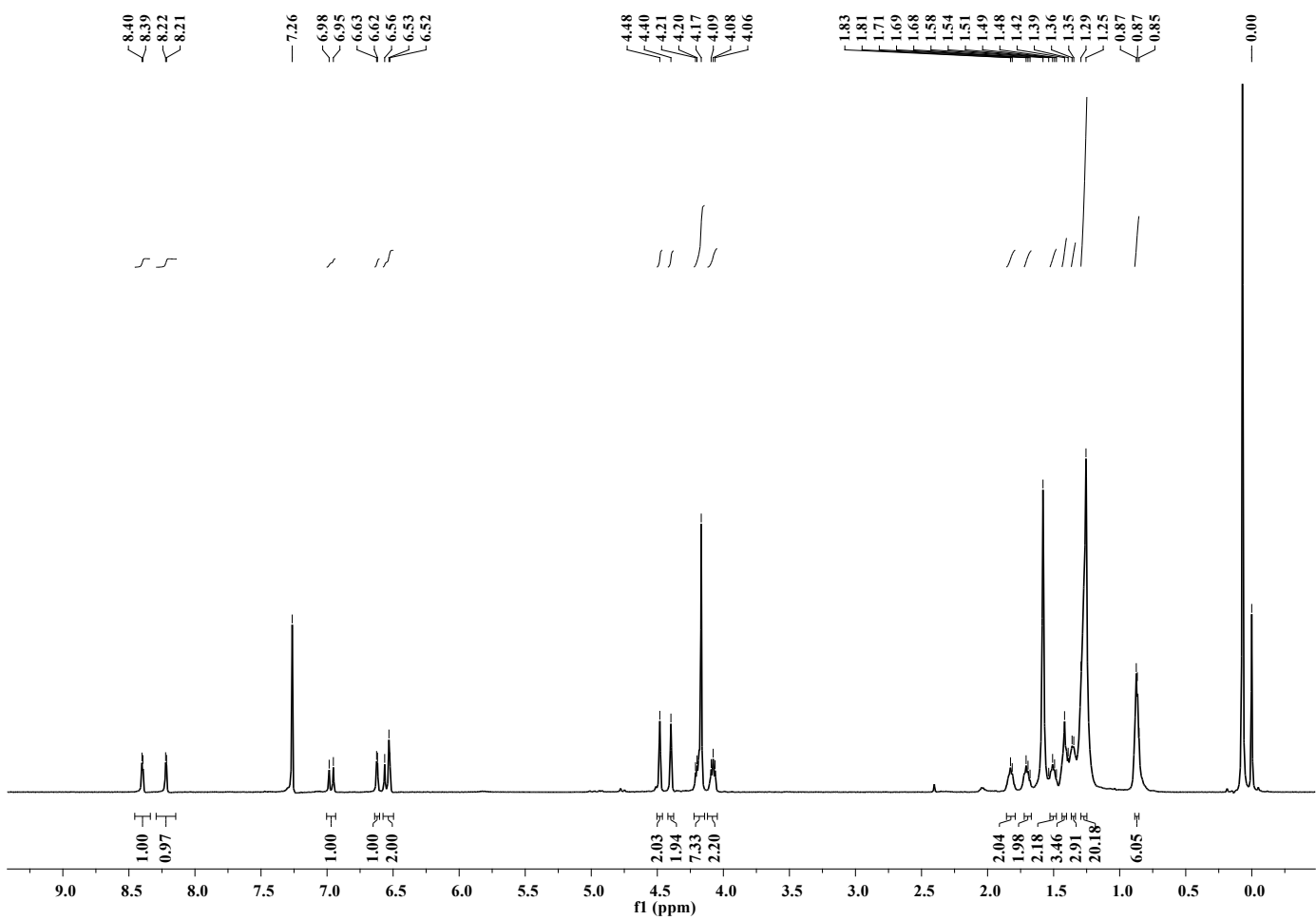


Figure S29. ^1H NMR of **5a** (CDCl_3 , 500 MHz).

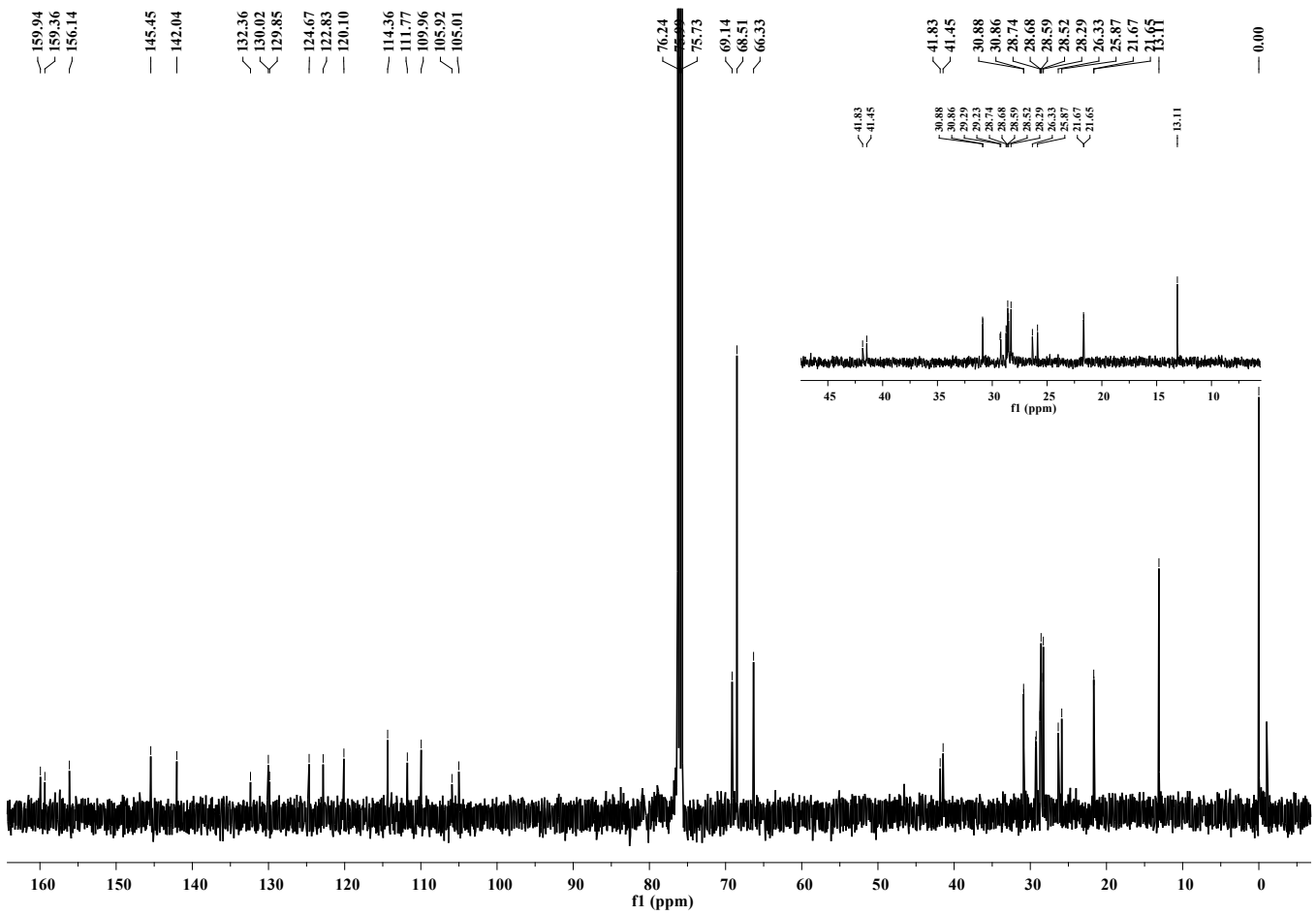


Figure S30. ^{13}C NMR of **5a** (CDCl_3 , 500 MHz). (Inset shows the expanded region from 10-45 ppm)

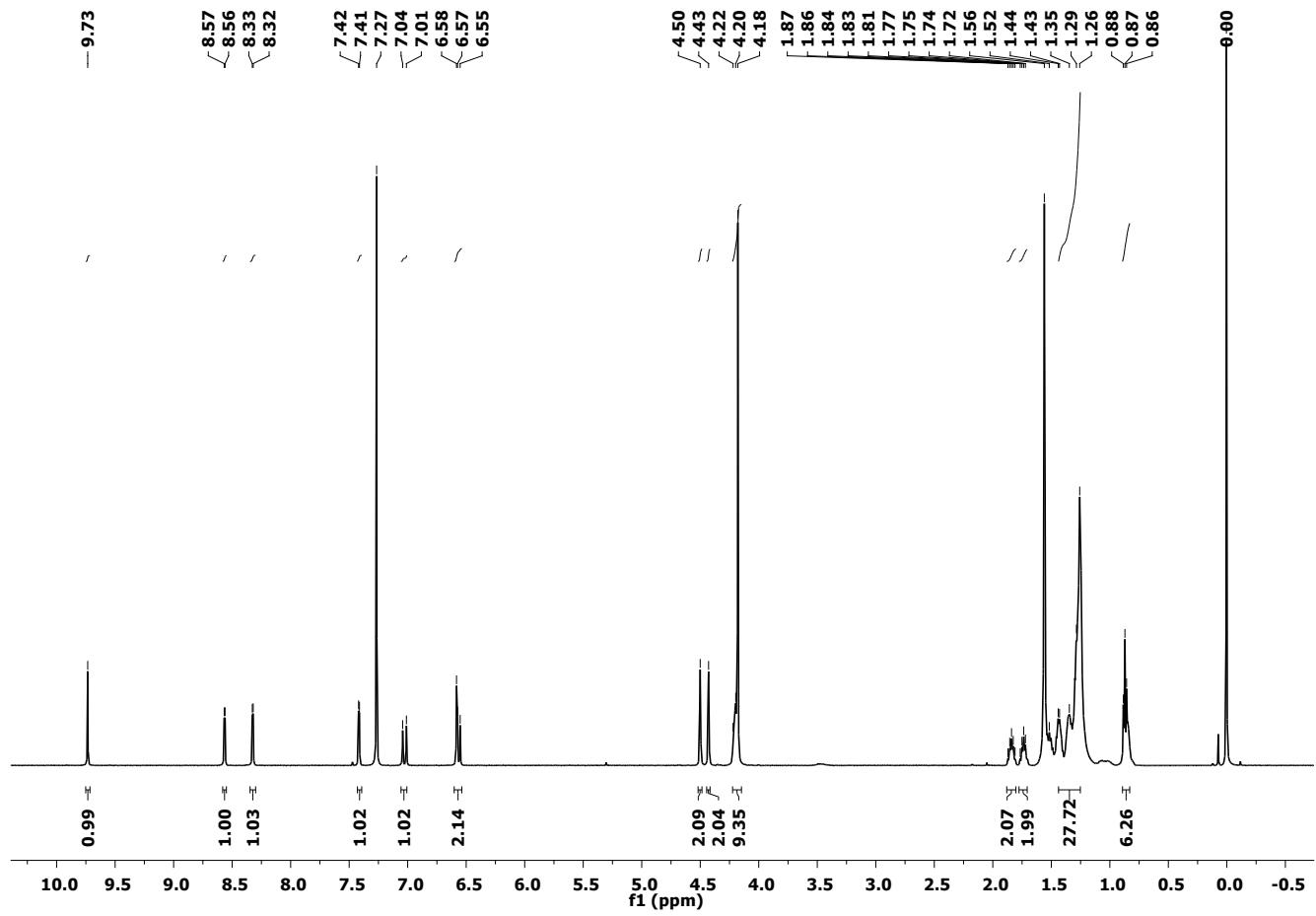


Figure S31. ${}^1\text{H}$ NMR of **5b** (CDCl_3 , 500 MHz).

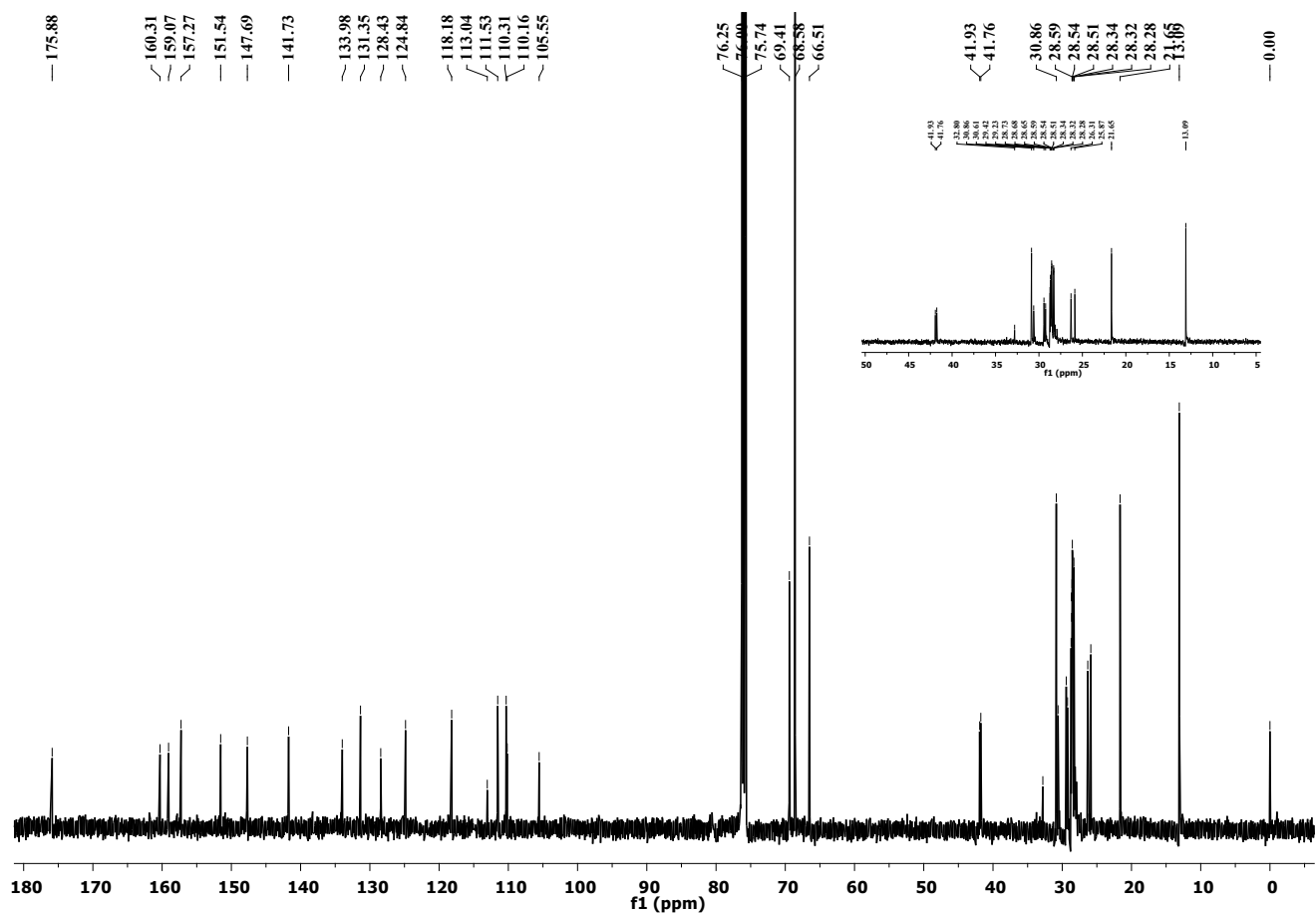


Figure S32. ^{13}C NMR of **5b** (CDCl_3 , 500 MHz). (Inset shows the expanded region from 10-50 ppm)

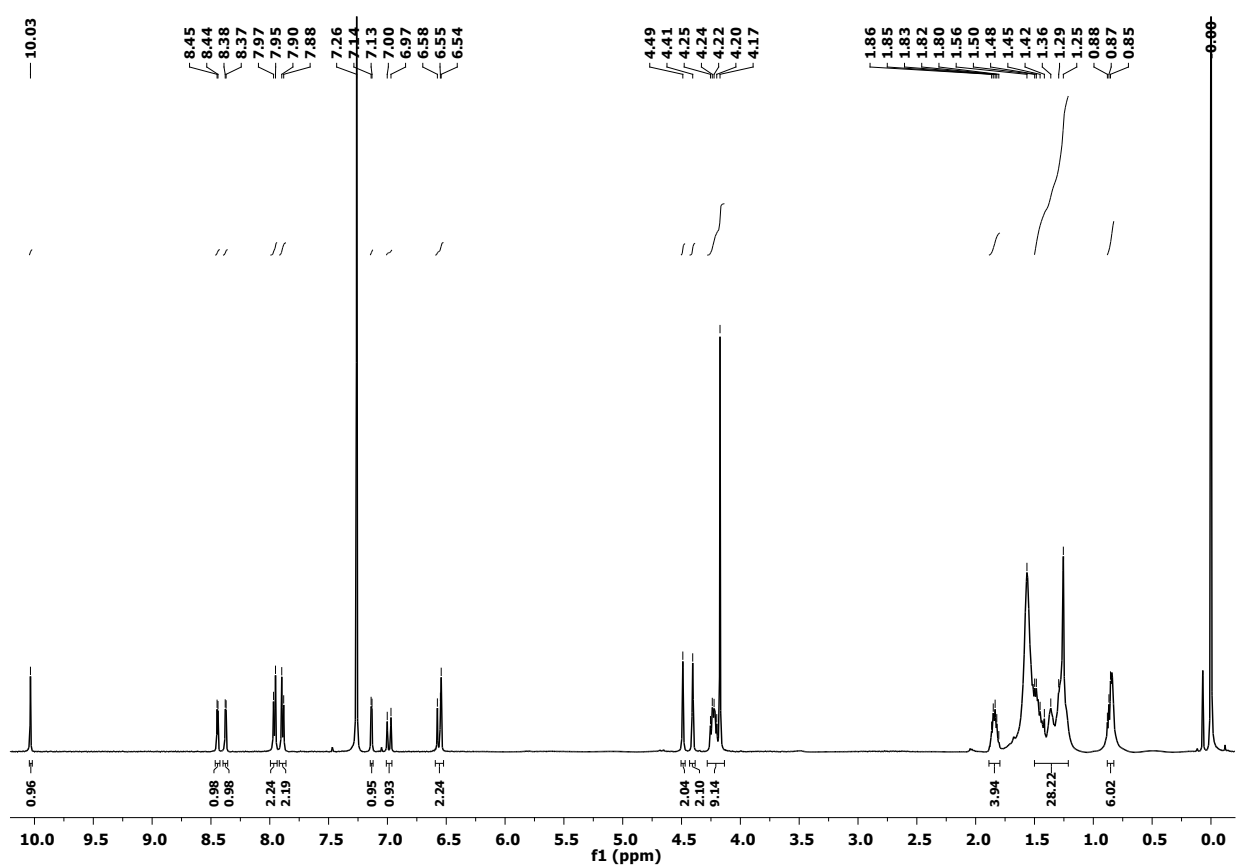
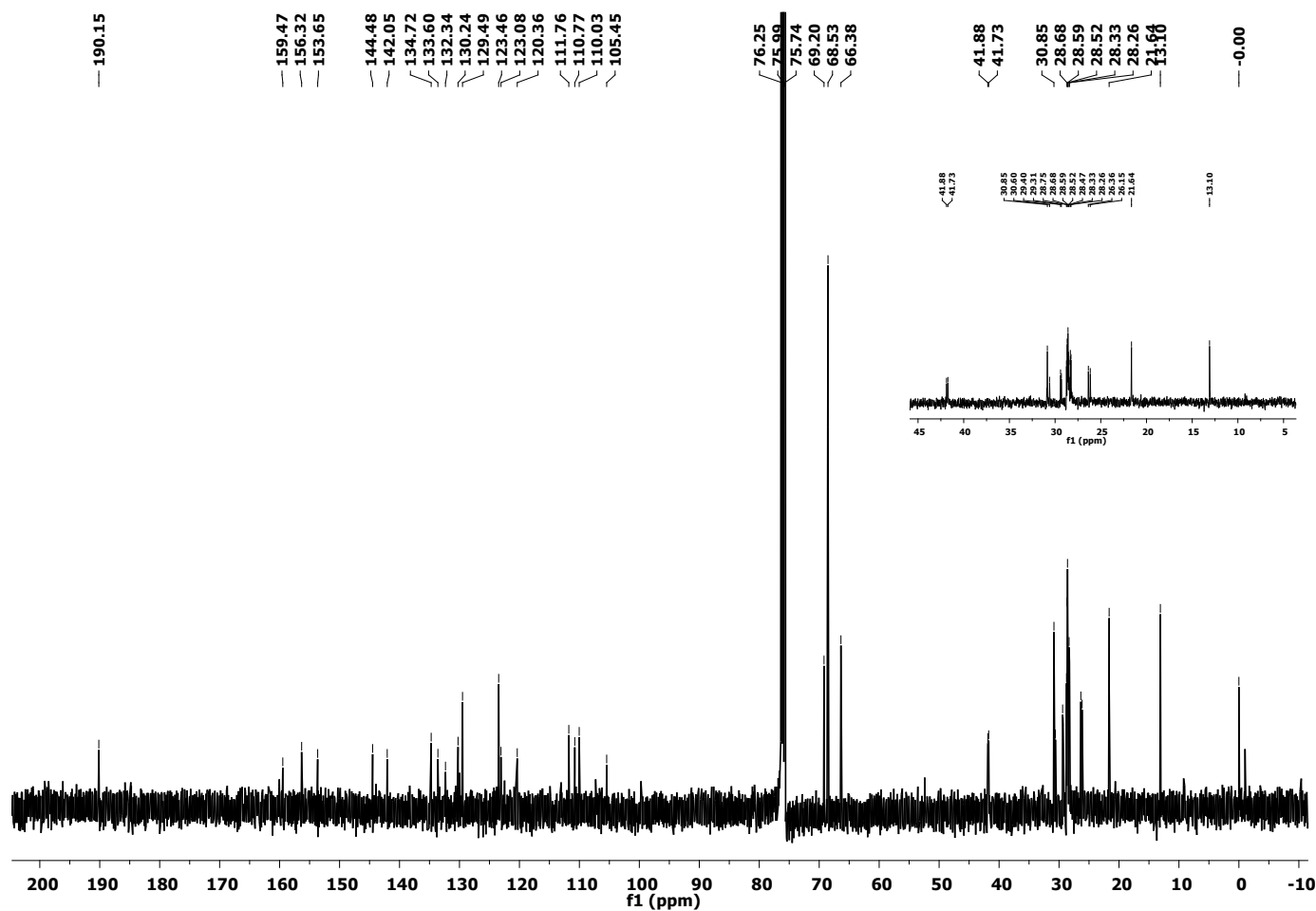


Figure S33. ^1H NMR of **5c** (CDCl_3 , 500 MHz).



— 190.15
— 159.47
— 144.48
— 142.05
— 134.72
— 133.60
— 132.34
— 130.24
— 129.49
— 123.46
— 123.08
— 123.06
— 111.76
— 110.77
— 110.03
— 105.45

— 76.25
— 75.99
— 75.74
— 69.20
— 68.53
— 66.38
— 41.88
— 41.73
— 41.38
— 30.85
— 30.40
— 29.40
— 29.21
— 29.12
— 28.68
— 28.59
— 28.52
— 28.47
— 28.33
— 28.26
— 28.20
— 28.14
— 28.07
— 28.00
— 27.93
— 27.86
— 27.79
— 27.72
— 27.65
— 27.58
— 27.51
— 27.44
— 27.37
— 27.30
— 27.23
— 27.16
— 27.09
— 27.02
— 26.95
— 26.88
— 26.81
— 26.74
— 26.

7	1	0	-8.796216	-5.642053	-1.600177
8	6	0	-8.166002	-3.507102	-1.897384
9	1	0	-9.025725	-3.063214	-2.374309
10	6	0	-8.140592	-2.039539	1.471295
11	1	0	-7.881157	-1.004154	1.316154
12	6	0	-7.310105	-3.033438	2.088174
13	1	0	-6.312198	-2.877099	2.467152
14	6	0	-8.038161	-4.270077	2.110283
15	1	0	-7.688159	-5.204845	2.519297
16	6	0	-9.321091	-4.039565	1.509211
17	1	0	-10.104111	-4.771175	1.385774
18	6	0	-9.384529	-2.661406	1.114048
19	1	0	-10.224534	-2.175025	0.643468
20	1	0	-6.731489	-1.793410	-1.766667
21	6	0	-4.674017	-3.584173	-0.537358
22	1	0	-4.217823	-4.424919	-0.016578
23	6	0	-3.936398	-2.463772	-0.748288
24	1	0	-4.365408	-1.621404	-1.282920
25	6	0	-0.675145	-1.071584	-0.165975
26	6	0	-2.579030	-2.284640	-0.324655
27	6	0	-1.638678	-3.049460	0.351642
28	8	0	-1.992549	-1.053196	-0.649957
29	6	0	-0.445071	-2.293972	0.452208
30	1	0	-1.792961	-4.047006	0.731568
31	1	0	0.490192	-2.579289	0.914440
32	6	0	0.183742	0.045882	-0.342384
33	6	0	1.510580	0.140414	0.086557
34	6	0	0.997420	2.149402	-0.970210
35	6	0	2.027733	1.411928	-0.284796
36	6	0	2.540508	-0.595476	0.771166
37	6	0	3.351965	1.506771	0.140446
38	8	0	2.574862	-1.740125	1.284969
39	8	0	0.967505	3.295993	-1.478794
40	7	0	-0.130043	1.252619	-0.984673
41	7	0	3.669920	0.304239	0.781959
42	6	0	-1.406842	1.674817	-1.575277
43	1	0	-1.149830	2.457625	-2.295175
44	1	0	-1.843288	0.830560	-2.112236
45	6	0	-2.400932	2.227755	-0.538938
46	1	0	-2.593680	1.461756	0.222996
47	1	0	-1.941264	3.085779	-0.030480
48	6	0	-3.729673	2.655218	-1.187134
49	1	0	-3.533017	3.406023	-1.967486
50	1	0	-4.180555	1.789562	-1.697191
51	6	0	-4.738254	3.228045	-0.174563
52	1	0	-4.293170	4.102396	0.323840
53	1	0	-4.920610	2.483645	0.615757
54	6	0	-6.080662	3.633095	-0.809745

55	1	0	-6.525895	2.757372	-1.307397
56	1	0	-5.898877	4.376051	-1.601358
57	6	0	-7.087839	4.206698	0.203675
58	1	0	-6.646414	5.087869	0.693933
59	1	0	-7.261431	3.467364	1.000942
60	6	0	-8.436688	4.598476	-0.426399
61	1	0	-8.878119	3.716656	-0.916370
62	1	0	-8.263910	5.337809	-1.223594
63	6	0	-9.443094	5.171439	0.587912
64	1	0	-9.004824	6.056536	1.074359
65	1	0	-9.612586	4.434350	1.388178
66	6	0	-10.795628	5.556230	-0.039353
67	1	0	-11.232166	4.671497	-0.526318
68	1	0	-10.626520	6.293447	-0.838113
69	6	0	-11.794034	6.125191	0.981627
70	1	0	-11.396222	7.029260	1.459634
71	1	0	-12.746306	6.389086	0.507048
72	1	0	-12.005406	5.396254	1.774230
73	6	0	4.947525	-0.112555	1.375778
74	1	0	5.377049	0.731590	1.918871
75	1	0	4.691441	-0.899050	2.091833
76	6	0	5.951458	-0.655103	0.343353
77	1	0	5.515632	-1.536309	-0.146161
78	1	0	6.117868	0.101186	-0.434279
79	6	0	7.296246	-1.024891	0.993931
80	1	0	7.126912	-1.758081	1.797328
81	1	0	7.722954	-0.130334	1.472753
82	6	0	8.315730	-1.596880	-0.007975
83	1	0	7.894973	-2.497853	-0.479713
84	1	0	8.473490	-0.869290	-0.818741
85	6	0	9.671744	-1.943167	0.633077
86	1	0	9.515205	-2.671710	1.443444
87	1	0	10.089078	-1.041296	1.106946
88	6	0	10.695354	-2.509079	-0.367991
89	1	0	10.282013	-3.415354	-0.836788
90	1	0	10.845416	-1.783357	-1.182190
91	6	0	12.055966	-2.842560	0.270380
92	1	0	12.467536	-1.935940	0.740393
93	1	0	11.906851	-3.569291	1.083874
94	6	0	13.081727	-3.404516	-0.730511
95	1	0	12.673145	-4.313564	-1.198477
96	1	0	13.228866	-2.679429	-1.545983
97	6	0	14.444838	-3.732024	-0.093624
98	1	0	14.851423	-2.823626	0.375227
99	1	0	14.298031	-4.457523	0.720180
100	6	0	15.463324	-4.289545	-1.100984
101	1	0	16.422374	-4.513471	-0.619457
102	1	0	15.095514	-5.215244	-1.561410

103	1	0	15.653443	-3.570331	-1.907735
104	6	0	4.208970	2.631760	-0.042421
105	6	0	6.095197	3.821089	0.103499
106	6	0	5.191585	4.609231	-0.551015
107	1	0	5.368105	5.606264	-0.918873
108	6	0	3.981505	3.853545	-0.647955
109	1	0	3.045761	4.148671	-1.102803
110	8	0	5.538201	2.598841	0.434782
111	35	0	7.894468	4.104203	0.608805

Table S7. Cartesian co-ordinates of optimized geometry (B3LYP/6-31G) of **5b**.

Center	Atomic Number	Atomic Number	Type	Coordinates (Angstroms)		
	X	Y	Z			
1	26	0	-7.387338	-3.692064	0.133910	
2	6	0	-6.676358	-2.627891	-1.497323	
3	6	0	-5.712322	-3.639478	-1.120874	
4	6	0	-6.389537	-4.916971	-1.204378	
5	1	0	-5.938828	-5.875883	-0.999068	
6	6	0	-7.727419	-4.692753	-1.657472	
7	1	0	-8.470965	-5.452614	-1.839002	
8	6	0	-7.903826	-3.279834	-1.839342	
9	1	0	-8.805508	-2.793263	-2.176474	
10	6	0	-7.733141	-2.344560	1.684489	
11	1	0	-7.576693	-1.277808	1.654728	
12	6	0	-6.769877	-3.326367	2.091104	
13	1	0	-5.759067	-3.126127	2.410584	
14	6	0	-7.386066	-4.619426	1.998575	
15	1	0	-6.923878	-5.561885	2.246778	
16	6	0	-8.732812	-4.435774	1.537507	
17	1	0	-9.460242	-5.216136	1.377644	
18	6	0	-8.947242	-3.030318	1.342354	
19	1	0	-9.864261	-2.569130	1.010862	
20	1	0	-6.495857	-1.565274	-1.538080	
21	6	0	-4.323917	-3.461299	-0.747833	
22	1	0	-3.825004	-4.348619	-0.360445	
23	6	0	-3.616548	-2.306941	-0.860194	
24	1	0	-4.083117	-1.419108	-1.276625	
25	6	0	-0.348871	-0.935352	-0.268265	
26	6	0	-2.247542	-2.148642	-0.469443	
27	6	0	-1.286760	-2.952218	0.131870	
28	8	0	-1.677250	-0.893972	-0.721806	
29	6	0	-0.097662	-2.196853	0.259599	
30	1	0	-1.428449	-3.972876	0.450099	

31	1	0	0.848081	-2.502810	0.686756
32	6	0	0.498853	0.195550	-0.380252
33	6	0	1.825794	0.274787	0.059373
34	6	0	1.297424	2.335399	-0.883921
35	6	0	2.333627	1.566379	-0.234406
36	6	0	2.856615	-0.493035	0.712512
37	6	0	3.653039	1.645343	0.208884
38	8	0	2.888792	-1.665368	1.158905
39	8	0	1.263131	3.507265	-1.324970
40	7	0	0.177492	1.433235	-0.954669
41	7	0	3.975458	0.411349	0.785477
42	6	0	-1.097540	1.873535	-1.537602
43	1	0	-0.839513	2.680488	-2.230008
44	1	0	-1.527844	1.046451	-2.105244
45	6	0	-2.099258	2.388542	-0.489435
46	1	0	-2.293582	1.597387	0.245979
47	1	0	-1.646197	3.231385	0.049298
48	6	0	-3.425266	2.831607	-1.132949
49	1	0	-3.225086	3.601204	-1.893850
50	1	0	-3.873345	1.978632	-1.666273
51	6	0	-4.439102	3.380187	-0.112260
52	1	0	-3.998712	4.245741	0.405202
53	1	0	-4.622134	2.619517	0.662261
54	6	0	-5.780230	3.793375	-0.744973
55	1	0	-6.222805	2.924816	-1.257283
56	1	0	-5.597002	4.548485	-1.524650
57	6	0	-6.791401	4.350527	0.273586
58	1	0	-6.354180	5.227089	0.775668
59	1	0	-6.964219	3.600713	1.061176
60	6	0	-8.140132	4.745184	-0.354998
61	1	0	-8.578558	3.867018	-0.854119
62	1	0	-7.967730	5.492457	-1.144825
63	6	0	-9.149780	5.306251	0.662699
64	1	0	-8.715265	6.188884	1.156878
65	1	0	-9.317830	4.562112	1.456753
66	6	0	-10.502782	5.691348	0.036590
67	1	0	-10.936101	4.808723	-0.457020
68	1	0	-10.334985	6.434593	-0.756830
69	6	0	-11.504044	6.250290	1.060275
70	1	0	-11.109714	7.152502	1.544587
71	1	0	-12.456635	6.514182	0.586388
72	1	0	-11.713950	5.515508	1.847867
73	6	0	5.252613	-0.007655	1.385439
74	1	0	5.636545	0.813443	1.993751
75	1	0	5.003667	-0.845959	2.042254
76	6	0	6.308665	-0.439990	0.351558
77	1	0	6.000820	-1.392856	-0.100010
78	1	0	6.353639	0.302025	-0.455226
79	6	0	7.703233	-0.568835	0.991051
80	1	0	7.650242	-1.239647	1.862840
81	1	0	8.010681	0.418721	1.364023
82	6	0	8.768948	-1.095080	0.013119

83	1	0	8.468580	-2.087033	-0.358669
84	1	0	8.809106	-0.434072	-0.866297
85	6	0	10.172169	-1.187638	0.639329
86	1	0	10.133282	-1.847009	1.520361
87	1	0	10.466857	-0.194506	1.009846
88	6	0	11.244553	-1.706842	-0.335387
89	1	0	10.947517	-2.699342	-0.708572
90	1	0	11.284072	-1.046792	-1.215746
91	6	0	12.647726	-1.799693	0.291230
92	1	0	12.943433	-0.807478	0.665296
93	1	0	12.608603	-2.460257	1.171280
94	6	0	13.722222	-2.315701	-0.682766
95	1	0	13.426948	-3.307958	-1.058001
96	1	0	13.763022	-1.654853	-1.562638
97	6	0	15.125455	-2.409219	-0.055693
98	1	0	15.419299	-1.417805	0.319723
99	1	0	15.084652	-3.069811	0.823080
100	6	0	16.192313	-2.923685	-1.035436
101	1	0	17.179170	-2.979318	-0.561101
102	1	0	15.939832	-3.926831	-1.401956
103	1	0	16.276993	-2.263337	-1.907880
104	6	0	4.513923	2.776951	0.101308
105	6	0	6.424676	3.934610	0.329207
106	6	0	5.501631	4.766875	-0.282380
107	1	0	5.681847	5.785596	-0.590522
108	6	0	4.291955	4.043042	-0.431150
109	1	0	3.360492	4.372010	-0.869557
110	8	0	5.820781	2.698487	0.572804
111	6	0	7.801343	4.125391	0.712466
112	1	0	8.189587	5.133543	0.488514
113	8	0	8.529093	3.265591	1.247046

Table S8. Cartesian co-ordinates of optimized geometry (B3LYP/6-31G) of **5c**

Center Number	Atomic Number	Atomic Type	Coordinates (Angstroms)		
			X	Y	Z
1	26	0	-8.477150	-3.435772	0.353133
2	6	0	-7.661722	-2.693567	-1.402146
3	6	0	-6.777691	-3.694803	-0.845431
4	6	0	-7.541478	-4.920927	-0.747273
5	1	0	-7.162931	-5.862776	-0.380471
6	6	0	-8.852564	-4.683041	-1.267786
7	1	0	-9.643880	-5.411148	-1.350543
8	6	0	-8.925862	-3.308060	-1.673408
9	1	0	-9.784229	-2.821882	-2.109761
10	6	0	-8.712122	-1.845703	1.676819
11	1	0	-8.442769	-0.816605	1.498442
12	6	0	-7.868103	-2.849444	2.257961
13	1	0	-6.848543	-2.708619	2.581271

14	6	0	-8.616587	-4.071946	2.331504
15	1	0	-8.262920	-5.009163	2.731625
16	6	0	-9.925455	-3.822614	1.797778
17	1	0	-10.727392	-4.540209	1.723776
18	6	0	-9.984565	-2.447094	1.392780
19	1	0	-10.839284	-1.949236	0.962473
20	1	0	-7.406336	-1.665720	-1.606599
21	6	0	-5.384628	-3.555735	-0.470974
22	1	0	-4.947734	-4.416548	0.033350
23	6	0	-4.604559	-2.470743	-0.713463
24	1	0	-5.014217	-1.610190	-1.234018
25	6	0	-1.267057	-1.225332	-0.242270
26	6	0	-3.226952	-2.352752	-0.337631
27	6	0	-2.302164	-3.155233	0.317127
28	8	0	-2.595622	-1.151596	-0.689686
29	6	0	-1.074215	-2.453585	0.378351
30	1	0	-2.490404	-4.141845	0.709994
31	1	0	-0.140423	-2.776690	0.818214
32	6	0	-0.367288	-0.146527	-0.445579
33	6	0	0.970765	-0.101981	-0.039705
34	6	0	0.520690	1.916013	-1.104607
35	6	0	1.533196	1.143275	-0.428572
36	6	0	1.978566	-0.874490	0.636602
37	6	0	2.868123	1.189042	-0.021532
38	8	0	1.973006	-2.016731	1.157494
39	8	0	0.527415	3.057287	-1.624624
40	7	0	-0.642505	1.065910	-1.092655
41	7	0	3.143393	-0.022910	0.625710
42	6	0	-1.907619	1.533968	-1.674582
43	1	0	-1.625574	2.298768	-2.404380
44	1	0	-2.383049	0.703216	-2.199673
45	6	0	-2.868671	2.138859	-0.636271
46	1	0	-3.117745	1.378504	0.114681
47	1	0	-2.355847	2.958103	-0.114893
48	6	0	-4.159247	2.665644	-1.288754
49	1	0	-3.903204	3.425000	-2.043055
50	1	0	-4.655908	1.846016	-1.831312
51	6	0	-5.145866	3.271683	-0.273761
52	1	0	-4.644733	4.080841	0.278668
53	1	0	-5.412286	2.508509	0.473538
54	6	0	-6.429715	3.819995	-0.922373
55	1	0	-6.926921	3.014216	-1.484650
56	1	0	-6.161170	4.589528	-1.662144
57	6	0	-7.421370	4.416386	0.093346
58	1	0	-6.920629	5.214541	0.662475
59	1	0	-7.698318	3.643957	0.827451
60	6	0	-8.697923	4.981152	-0.555741
61	1	0	-9.197092	4.184993	-1.129668
62	1	0	-8.420033	5.757131	-1.285462
63	6	0	-9.691518	5.572811	0.460654
64	1	0	-9.191388	6.365453	1.038324
65	1	0	-9.974711	4.795876	1.187627

66	6	0	-10.964477	6.146630	-0.188350
67	1	0	-11.463608	5.354834	-0.766498
68	1	0	-10.680356	6.923177	-0.913834
69	6	0	-11.950241	6.734657	0.834184
70	1	0	-11.486436	7.549139	1.404811
71	1	0	-12.844398	7.136694	0.343759
72	1	0	-12.276433	5.970843	1.551385
73	6	0	4.406243	-0.496306	1.206018
74	1	0	4.883515	0.330196	1.736919
75	1	0	4.120150	-1.262814	1.932551
76	6	0	5.364936	-1.104199	0.166835
77	1	0	4.839264	-1.904602	-0.370439
78	1	0	5.636210	-0.339247	-0.571983
79	6	0	6.637508	-1.670759	0.821596
80	1	0	6.356857	-2.438864	1.557977
81	1	0	7.147000	-0.874306	1.387257
82	6	0	7.623228	-2.276451	-0.194380
83	1	0	7.111938	-3.064558	-0.767459
84	1	0	7.913592	-1.504563	-0.923247
85	6	0	8.888119	-2.862752	0.458134
86	1	0	8.595804	-3.638982	1.181834
87	1	0	9.395966	-2.077006	1.038953
88	6	0	9.878515	-3.461949	-0.557110
89	1	0	9.368769	-4.241917	-1.143258
90	1	0	10.177260	-2.683552	-1.275957
91	6	0	11.137501	-4.060117	0.096290
92	1	0	11.646087	-3.281463	0.685632
93	1	0	10.837853	-4.840645	0.812558
94	6	0	12.129708	-4.656606	-0.918597
95	1	0	11.620838	-5.432505	-1.511258
96	1	0	12.433869	-3.875484	-1.632395
97	6	0	13.385707	-5.261816	-0.265134
98	1	0	13.894023	-4.486390	0.326887
99	1	0	13.080627	-6.041670	0.448314
100	6	0	14.369820	-5.855755	-1.285804
101	1	0	15.251173	-6.281409	-0.792124
102	1	0	13.895883	-6.653608	-1.871486
103	1	0	14.717896	-5.089254	-1.989666
104	6	0	3.764577	2.276898	-0.224281
105	6	0	5.711211	3.421358	-0.119007
106	6	0	4.787310	4.212995	-0.776857
107	1	0	4.964387	5.201512	-1.169638
108	6	0	3.562758	3.500014	-0.846196
109	1	0	2.629305	3.816203	-1.290895
110	8	0	5.089925	2.214436	0.230401
111	6	0	7.099522	3.595303	0.249404
112	6	0	7.800983	2.585698	0.944881
113	6	0	7.779496	4.792088	-0.085920
114	6	0	9.136033	2.770294	1.291205
115	1	0	7.289163	1.667371	1.204498
116	6	0	9.110560	4.969563	0.261922
117	1	0	7.255459	5.576867	-0.620381

118	6	0	9.806688	3.959460	0.955891
119	1	0	9.668858	1.988663	1.826282
120	1	0	9.638932	5.882252	0.008701
121	6	0	11.216759	4.140839	1.326625
122	1	0	11.674845	3.293079	1.868743
123	8	0	11.889263	5.155484	1.071524

Complete reference 75.

Gaussian 09, Revision B.01, M. J. Frisch, G. W. Trucks, H. B. Schlegel, G. E. Scuseria, M. A. Robb, J. R. Cheeseman, G. Scalmani, V. Barone, B. Mennucci, G. A. Petersson, H. Nakatsuji, M. Caricato, X. Li, H. P. Hratchian, A. F. Izmaylov, J. Bloino, G. Zheng, J. L. Sonnenberg, M. Hada, M. Ehara, K. Toyota, R. Fukuda, J. Hasegawa, M. Ishida, T. Nakajima, Y. Honda, O. Kitao, H. Nakai, T. Vreven, J. A. Montgomery, Jr., J. E. Peralta, F. Ogliaro, M. Bearpark, J. J. Heyd, E. Brothers, K. N. Kudin, V. N. Staroverov, T. Keith, R. Kobayashi, J. Normand, K. Raghavachari, A. Rendell, J. C. Burant, S. S. Iyengar, J. Tomasi, M. Cossi, N. Rega, J. M. Millam, M. Klene, J. E. Knox, J. B. Cross, V. Bakken, C. Adamo, J. Jaramillo, R. Gomperts, R. E. Stratmann, O. Yazyev, A. J. Austin, R. Cammi, C. Pomelli, J. W. Ochterski, R. L. Martin, K. Morokuma, V. G. Zakrzewski, G. A. Voth, P. Salvador, J. J. Dannenberg, S. Dapprich, A. D. Daniels, O. Farkas, J. B. Foresman, J. V. Ortiz, J. Cioslowski, and D. J. Fox, Gaussian, Inc., Wallingford CT, 2010.(complete reference 75).